NORSAR Scientific Report No. 2-2005

Semiannual Technical Summary

1 January - 30 June 2005

Frode Ringdal (ed.)

Kjeller, August 2005

REPORT DOCUMENTATION PAGE

Form Approved
OMB No. 0704-0188

1. REPORT DATE *(DD-MM-YYYY)*	2. REPORT TYPE	3. DATES COVERED *(From - To)*
15 August 2005	Semiannual Technical Summary	1 January - 30 June 2005

4. TITLE AND SUBTITLE
Semiannual Technical Summary, 1 January - 30 June 2005

5a. CONTRACT NUMBER
F08650-01-C-0055

5b. GRANT NUMBER

5c. PROGRAM ELEMENT NUMBER
NDC Support / R&D

6. AUTHOR(S)
Frode Ringdal (Ed.)

5d. PROJECT NUMBER
T/0155, NORSAR Phase 3

5e. TASK NUMBER
SOW Task 4.3

5f. WORK UNIT NUMBER
CDRL sequence nos. A001-A004

7. PERFORMING ORGANIZATION NAME(S) AND ADDRESS(ES)
Stiftelsen NORSAR
Post Box 53
NO-2027 Kjeller
Norway

8. PERFORMING ORGANIZATION REPORT NUMBER
Scientific Report No. 2-2005

9. SPONSORING/MONITORING AGENCY NAME(S) AND ADDRESS(ES)
Army Space and Missile Defense Command
1515 Wilson Blvd., Suite 720
Arlington, VA 22209

10. SPONSOR/MONITOR'S ACRONYM(S)
ASMDC

11. SPONSOR/MONITOR'S REPORT NUMBER(S)

12. DISTRIBUTION/AVAILABILITY STATEMENT
Approved for public release; distribution unlimited

13. SUPPLEMENTARY NOTES

14. ABSTRACT

This report describes the research activities carried out at NORSAR under Contract No. F085650-01-C-0055 for the period 1 January - 30 June 2005. In addition, it provides summary information on operation and maintenance (O&M) activities at the Norwegian National Data Center (NDC) during the same period. Research activities described in this report are largely funded by the United States Government, and the United States also covers the cost of transmission of selected data to the United States NDC. The O&M activities, including operation and transmission links within Norway and to Vienna, Austria, are being funded jointly by the CTBTO/PTS and the Norwegian Government, with the understanding that the funding of O&M activities for primary IMS will gradually be transferred to the CTBTO/PTS. The O&M statistics presented in this report are included for the purpose of completeness, and in order to maintain consistency with earlier reporting practice.
(cont.)

15. SUBJECT TERMS
NORSAR, Norwegian Seismic Array

16. SECURITY CLASSIFICATION OF:			17. LIMITATION OF ABSTRACT	18. NUMBER OF PAGES	19a. NAME OF RESPONSIBLE PERSON
a. REPORT	b. ABSTRACT	c. THIS PAGE			SSgt Mark LeDoux, AFTAC/TTS
U	U	U	SAR	60	19b. TELEPHONE NUMBER *(Include area code)* (321) 494-9471

Reset

Standard Form 298 (Rev. 8/98)
Prescribed by ANSI Std. Z39.18

Abstract (continued)

The NOA Detection Processing system has been operated throughout the period with an uptime of 100%. A total of 3240 seismic events have been reported in the NOA monthly seismic bulletin during the reporting period. On-line detection processing and data recording at the NDC of data from ARCES, FINES, SPITS and HFS data have been conducted throughout the period. Processing statistics for the arrays for the reporting period are given.

A summary of the activities at the Norwegian NDC and relating to field installations during the reporting period is provided in Section 4. Norway is now contributing primary station data from two seismic arrays: NOA (PS27) and ARCES (PS28) one auxiliary seismic array SPITS (AS72) and one auxiliary three-component station (JMIC). These data are being provided to the IDC via the global communications infrastructure (GCI). Continuous data from the three arrays are in addition being transmitted to the US NDC. The performance of the data transmission to the US NDC has been satisfactory during the reporting period.

Summaries of four scientific and technical contributions are presented in Section 6 of this report.

Section 6.1 is entitled "Detecting the aftershock of the 16 August 1997 Kara Sea event by waveform correlation". The paper describes an initial investigation of the potential of obtaining improved detection of small seismic events by the use of waveform correlation in conjunction with array processing. We have used as an example the small aftershock (m_b=2.5) which occurred about 4 hours after the 16 August 1997 Kara Sea event, using data from three stations: the Amderma station in northerh Russia (distance 325 km), the SPITS array (distance 1100 km) and the large NORSAR array (NOA), at a distance of 2300 km. The most impressive result is the processing of the data recorded by the large aperture NORSAR array at a distance of approximately 2300 km from the source. No detection by traditional processing is possible at this array for the signal from the second event. Cross-correlating one minute long data segments from the main event with the corresponding waveforms from the time of the second event does not result in peaks on single-sensor correlation-traces which allow detection of the event. However, the event is clearly detectable on the NORSAR array by stacking the correlation coefficient traces from the various sites. This is a superb demonstration of how the cross-correlation functions are coherent across a large array or network even when the actual waveforms are not.

Section 6.2 is entitled "Automatic real-time detection and processing of regional seismic phases on the wide-aperture NORSAR array". Such processing is notoriously difficult, due to the low coherency across the large array of the high-frequency regional phases, and has not been successfully implemented in the past. The paper describes a new, experimental, processing system for incorporating regional seismic phases detected by the large NORSAR (NOA) array into the Generalized Beamforming (GBF) process currently in use at NORSAR for on-line automatic detection and location of seismic events in the European Arctic. The contribution outlines a method of phase detection and parameter estimation based upon continuous spectral estimates which has proved to be remarkably robust and, although still in an experimental phase, provides a significant contribution to the online GBF. This is particularly important since the regional array NORES in southern Norway is no longer in operation, and the new process therefore contributes to filling the gap after NORES. The system represents a significant improvement over previous processing systems for large arrays, and we recommend that this

method be further developed for improving automatic detection and location using local or regional networks.

Section 6.3 is entitled "Surface Wave Tomography for the Barents Sea and Surrounding Regions". In this project, we have extensively searched for long period and broadband data observed at the seismic stations and arrays in the area from the beginning of the 1970s until 2005. We have been able to retrieve surface wave observations from the data archives at NORSAR, University of Bergen, the Kola Science Center in Apatity, the Geological Service of Denmark and the University of Helsinki, in addition to the data, retrieved from the international data centers IRIS and GEOFON. In these data archives, not yet analyzed Love- and Rayleigh-wave data were identified and for more than 150 seismic events (earthquakes and nuclear explosions) dispersion curves were measured. We have made a tomographic inversion for two-dimensional group-velocity maps for a set of periods between 14 and 90 seconds. In all cases, we inverted the combined data set of the newly acquired and analyzed data and a preselected data set from the University of Colorado. As first results, we present in this paper the resulting group-velocity maps for Love and Rayleigh waves at three different periods: 16, 25, and 40 s, respectively. These group-velocity maps show the lateral deviation of the group velocities from the average velocity in percent. We show that these deviations are up to ±36% for Love and Rayleigh waves with a period of 16 s. This reflects the strong lateral heterogeneity of the Earth's crust in this region, which changes between the mid-oceanic ridge system, the thick sedimentary basins in the Barents Sea, and the old continental shields.

Section 6.4 contains a continued study of combining seismic and infrasonic recordings for detection and characterization of seismic events at local and regional distances. We present results from an analysis of several recent surface explosions in the Kola peninsula near the Norwegian border. At least two of the explosions were reported felt/heard over a large area in the Varanger peninsula, northern Norway, at an epicentral distance of more than 100 km. These explosions were presumably carried out for the purpose of destroying old ammunition, and generated unusually strong infrasonic signals in addition to seismic signals. Not unexpectedly, the infrasonic signals were well recorded on the infrasound array in Apatity, but more interestingly, they were also clearly recorded on the seismic sensors at the ARCES and Apatity arrays (both at about 250 km distance from the source area). We used the estimated azimuths (from the infrasonic waves) for the two arrays to locate the six events, using the HYPOSAT program. For the Apatity array, we used the three infrasonic sensors, and for the ARCES array we used infrasonic observations on the seismic sensors. We found that the locations matched closely the locations obtained through standard seismic data analysis. This indicates an interesting potential for joint two-array seismic and infrasonic processing, and this concept will be further developed once the IMS infrasound array near ARCES has been established (expected in 2006).

AFTAC Project Authorization	:	T/0155/PKO
ARPA Order No.	:	4138 AMD # 53
Program Code No.	:	0F10
Name of Contractor	:	Stiftelsen NORSAR
Effective Date of Contract	:	1 Feb 2001 (T/0155/PKO)
Contract Expiration Date	:	31 December 2005
Project Manager	:	Frode Ringdal +47 63 80 59 00
Title of Work	:	The Norwegian Seismic Array (NORSAR) Phase 3
Amount of Contract	:	$ 2,879,151.06
Period Covered by Report	:	1 January - 30 June 2005

The views and conclusions contained in this document are those of the authors and should not be interpreted as necessarily representing the official policies, either expressed or implied, of the U.S. Government.

The research presented in this report was supported by the Army Space and Missile Defense Command and was monitored by AFTAC, Patrick AFB, FL32925, under contract no. F08650-01-C-0055.

The operational activities of the seismic field systems and the Norwegian National Data Center (NDC) are currently jointly funded by the Norwegian Government and the CTBTO/PTS, with the understanding that the funding of IMS-related activities will gradually be transferred to the CTBTO/PTS.

NORSAR Contribution No. 961

Table of Contents

Page

1 Summary

This report describes the research activities carried out at NORSAR under Contract No. F08650-01-C-0055 for the period 1 January - 30 June 2005. In addition, it provides summary information on operation and maintenance (O&M) activities at the Norwegian National Data Center (NDC) during the same period. Research activities described in this report are largely funded by the United States Government, and the United States also covers the cost of transmission of selected data to the US NDC. The O&M activities, including operation of transmission links within Norway and to Vienna, Austria are being funded jointly by the CTBTO/PTS and the Norwegian Government, with the understanding that the funding of O&M activities for primary stations in the International Monitoring System (IMS) will gradually be transferred to the CTBTO/PTS. The O&M statistics presented in this report are included for the purpose of completeness, and in order to maintain consistency with earlier reporting practice.

The seismic arrays operated by the Norwegian NDC comprise the Norwegian Seismic Array (NOA), the Arctic Regional Seismic Array (ARCES) and the Spitsbergen Regional Array (SPITS). This report presents statistics for these three arrays as well as for additional seismic stations which through cooperative agreements with institutions in the host countries provide continuous data to the NORSAR Data Processing Center (NDPC). These additional stations include the Finnish Regional Seismic Array (FINES) and the Hagfors array in Sweden (HFS).

The NOA Detection Processing system has been operated throughout the period with an uptime of 100%. A total of 3240 seismic events have been reported in the NOA monthly seismic bulletin during the reporting period. On-line detection processing and data recording at the NDC of data from ARCES, FINES, SPITS and HFS data have been conducted throughout the period. Processing statistics for the arrays for the reporting period are given.

A summary of the activities at the Norwegian NDC and relating to field installations during the reporting period is provided in Section 4. Norway is now contributing primary station data from two seismic arrays: NOA (PS27) and ARCES (PS28) one auxiliary seismic array SPITS (AS72) and one auxiliary three-component station (JMIC). These data are being provided to the IDC via the global communications infrastructure (GCI). Continuous data from the three arrays are in addition being transmitted to the US NDC. The performance of the data transmission to the US NDC has been satisfactory during the reporting period.

So far among the Norwegian stations, the NOA and the ARCES array (PS27 and PS28 respectively) and the radionuclide station at Spitsbergen (RN49) have been certified. Provided that adequate funding continues to be made available (from the PTS and the Norwegian Ministry of Foreign Affairs), we envisage continuing the provision of data from these and other Norwegian IMS-designated stations in accordance with current procedures. The IMS infrasound station at Karasjok (IS37) is expected to be built in 2006, provided adequate resources for project planning and execution are made available.

Summaries of four scientific and technical contributions are presented in Chapter 6 of this report.

Section 6.1 is entitled “Detecting the aftershock of the 16 August 1997 Kara Sea event by waveform correlation”. The paper describes an initial investigation of the potential of obtaining improved detection of small seismic events by the use of waveform correlation in conjunction with array processing. We have used as an example the small aftershock (m_b=2.5) which occurred about 4 hours after the 16 August 1997 Kara Sea event, using data from three stations:

the Amderma station in northerh Russia (distance 325 km), the SPITS array (distance 1100 km) and the large NORSAR array (NOA), at a distance of 2300 km.

At the Amderma station, the waveforms for both events exhibit a high SNR and there is a remarkable degree of waveform similarity between the two events. High correlation coefficients (~0.9) are obtained by correlating 60.0 second long data segments from the two events filtered between 4.0 and 8.0 Hz.

At the SPITS array, the detection of the second event using traditional array processing at the NORSAR Data Center was marginal, resulting only in several weak P-phase detections. We demonstrate that, using the signal from the main event as a waveform template, the second event is easily detected at SPITS using waveform correlation even on a single seismometer channel. The correlation coefficients observed on the individual channels are approximately 0.65 for one minute long data segments (between 4 and 8 Hz) which is remarkably high considering the low SNR of the signal from the second event. Performing waveform correlation over the whole array provides us with the useful observation that the times of maximum cross-correlation are the same for each array element which supports the claim that both signals come from approximately the same site.

The most impressive result is the processing of the data recorded by the large aperture NORSAR array at a distance of approximately 2300 km from the source. No detection by traditional processing is possible at this array for the signal from the second event. Cross-correlating one minute long data segments from the main event with the corresponding waveforms from the time of the second event does not result in peaks on single-sensor correlation-traces which allow detection of the event. However, the event is clearly detectable on the NORSAR array by stacking the correlation coefficient traces from the various sites. This is a superb demonstration of how the cross-correlation functions are coherent across a large array or network even when the actual waveforms are not.

It is noteworthy that the same time separation between the two events (14890.9 seconds) was obtained from cross-correlating the recordings at each of these three sites.

Section 6.2 is entitled “Automatic real-time detection and processing of regional seismic phases on the wide-aperture NORSAR array”. Such processing is notoriously difficult, due to the low coherency across the large array of the high-frequency regional phases, and has not been successfully implemented in the past. The paper describes a new, experimental, processing system for incorporating regional seismic phases detected by the large NORSAR (NOA) array into the Generalized Beamforming (GBF) process currently in use at NORSAR for on-line automatic detection and location of seismic events in the European Arctic.

The contribution outlines a method of phase detection and parameter estimation based upon continuous spectral estimates which has proved to be remarkably robust and, although still in an experimental phase, provides a significant contribution to the online GBF. This is particularly important since the regional array NORES in southern Norway is no longer in operation, and the new process therefore contributes to filling the gap after NORES. The system represents a significant improvement over previous processing systems for large arrays, and we recommend that this method be further developed for improving automatic detection and location using local or regional networks.

Section 6.3 is entitled “Surface Wave Tomography for the Barents Sea and Surrounding Regions”. Existing global and regional tomographic models have limited resolution in the

European Arctic due to the small number of seismic stations, relatively low regional seismicity, and limited knowledge of the crustal structure. During the last decades, new seismic stations have been permanently or temporarily installed in and around this region. However, many of the data from these stations are not easily accessible via the international data centers but only by direct request to the different data operators.

In this project, we have extensively searched for long period and broadband data observed at the seismic stations and arrays in the area from the beginning of the 1970s until 2005. We have been able to retrieve surface wave observations from the data archives at NORSAR, University of Bergen, the Kola Science Center in Apatity, the Geological Service of Denmark and the University of Helsinki, in addition to the data, retrieved from the international data centers IRIS and GEOFON. In these data archives, not yet analyzed Love- and Rayleigh-wave data were identified and for more than 150 seismic events (earthquakes and nuclear explosions) dispersion curves were measured.

We have made a tomographic inversion for two-dimensional group-velocity maps for a set of periods between 14 and 90 seconds. In all cases, we inverted the combined data set of the newly acquired and analyzed data and a preselected data set from the University of Colorado. As first results, we present in this paper the resulting group-velocity maps for Love and Rayleigh waves at three different periods: 16, 25, and 40 s, respectively. These group-velocity maps show the lateral deviation of the group velocities from the average velocity in percent. We show that these deviations are up to ±36% for Love and Rayleigh waves with a period of 16 s. This reflects the strong lateral heterogeneity of the Earth's crust in this region, which changes between the mid-oceanic ridge system, the thick sedimentary basins in the Barents Sea, and the old continental shields.

The planned next step will be an inversion of all group-velocity maps (Love and Rayleigh waves) into a 3D shear-velocity model for the whole region. As additional constraints for the inversion we will use the thickness of the sedimentary layers and the Moho depth, as recently derived in a joint project of the University of Oslo, NORSAR and the USGS. This should result in a new, robust 3D model of the velocities in the upper mantle beneath the greater Barents Sea region down to about 250 km.

Section 6.4 contains a continued study of combining seismic and infrasonic recordings for detection and characterization of seismic events at local and regional distances. We present results from an analysis of several recent surface explosions in the Kola peninsula near the Norwegian border. At least two of the explosions were reported felt/heard over a large area in the Varanger peninsula, northern Norway, at an epicentral distance of more than 100 km. These explosions were presumably carried out for the purpose of destroying old ammunition, and generated unusually strong infrasonic signals in addition to seismic signals. Not unexpectedly, the infrasonic signals were well recorded on the infrasound array in Apatity, but more interestingly, they were also clearly recorded on the seismic sensors at the ARCES and Apatity arrays (both at about 250 km distance from the source area).

The paper discusses some of the characteristics of the infrasonic recordings of these explosions. The explosions took place on three separate days, with two explosions per day, separated in time by only approximately one half hour. Therefore, the atmospheric conditions would have been essentially the same for each pair. Nevertheless, the infrasonic recordings for the two events on each day show clear differences, whereas the seismic recordings are similar.

We used the estimated azimuths (from the infrasonic waves) for the two arrays to locate the six events, using the HYPOSAT program. For the Apatity array, we used the three infrasonic sensors, and for the ARCES array we used infrasonic observations on the seismic sensors. We found that the locations matched closely the locations obtained through standard seismic data analysis. This indicates an interesting potential for joint two-array seismic and infrasonic processing, and this concept will be further developed once the IMS infrasound array near ARCES has been established (expected in 2006).

Frode Ringdal

2 Operation of International Monitoring System (IMS) Stations in Norway

2.1 PS27 — Primary Seismic Station NOA

The mission-capable data statistics were 100%, the same as for the previous reporting period. The net instrument availability was 99.901%.

There were no outages of all subarrays at the same time in the reporting period.

Monthly uptimes for the NORSAR on-line data recording task, taking into account all factors (field installations, transmissions line, data center operation) affecting this task were as follows:

		Mission Capable	Net instrument availability
January	:	100%	99.820%
February	:	100%	99.884%
March	:	100%	99.951%
April	:	100%	99.999%
May	:	100%	99.953%
June	:	100%	99.798%

J. Torstveit

NOA Event Detection Operation

In Table 2.1.1 some monthly statistics of the Detection and Event Processor operation are given. The table lists the total number of detections (DPX) triggered by the on-line detector, the total number of detections processed by the automatic event processor (EPX) and the total number of events accepted after analyst review (teleseismic phases, core phases and total).

	Total DPX	Total EPX	Accepted Events		Sum	Daily
			P-phases	Core Phases		
Jan	16,288	1,717	1,046	43	1,089	35.1
Feb	11,153	955	286	52	338	12.1
Mar	12,517	1,257	458	54	512	16.5
Apr	9,881	1,076	424	45	469	15.6
May	7,367	845	335	61	396	12.8
Jun	6,211	862	337	99	436	14.5
	63,417	6,712	2,886	354	3,240	17.8

Table 2.1.1. *Detection and Event Processor statistics, 1 January - 30 June 2005.*

NOA detections

The number of detections (phases) reported by the NORSAR detector during day 001, 2005, through day 181, 2005, was 63,417, giving an average of 350 detections per processed day (181 days processed).

B. Paulsen

U. Baadshaug

2.2 PS28 — Primary Seismic Station ARCES

The mission-capable data statistics were 98.197%, as compared to 99.65% for the previous reporting period. The net instrument availability was 99.996%.

The main outages in the period are presented in Table 2.2.1.

Day	Period
03/04	09.33 -
06/04	- 15.35
21/04	15.40 - 15.49
22/04	05.30 - 05.39

Table 2.2.1. *The main interruptions in recording of ARCES data at NDPC, 1 January - 30 June 2005.*

Monthly uptimes for the ARCES on-line data recording task, taking into account all factors (field installations, transmission lines, data center operation) affecting this task were as follows:

		Mission Capable	Net instrument availability
January	:	100%	99.442%
February	:	100%	98.629%
March	:	100%	99.846%
April	:	89.123%	88.673%
May	:	100%	98.032%
June	:	100%	95.866%

J. Torstveit

Event Detection Operation

ARCES detections

The number of detections (phases) reported during day 001, 2005, through day 181, 2005, was 178,966, giving an average of 1000 detections per processed day (179 days processed).

Events automatically located by ARCES

During days 001, 2005, through 181, 2005, 9,154 local and regional events were located by ARCES, based on automatic association of P- and S-type arrivals. This gives an average of 51.1 events per processed day (179 days processed). 57% of these events are within 300 km, and 84% of these events are within 1000 km.

U. Baadshaug

2.3 AS72 — Auxiliary Seismic Station Spitsbergen

The mission-capable data for the period were 100% as compared to 95.46% for the previous reporting period. The net instrument availability was 97.712%.

There were no outages of all instruments at the same time in the reporting period.

Monthly uptimes for the Spitsbergen on-line data recording task, taking into account all factors (field installations, transmissions line, data center operation) affecting this task were as follows:

		Mission Capable	Net instrument availability
January	:	100%	97.474%
February	:	100%	93.593%
March	:	100%	99.931%
April	:	100%	99.867%
May	:	100%	95.154%
June	:	100%	99.996%

J. Torstveit

Event Detection Operation

Spitsbergen array detections

The number of detections (phases) reported from day 001, 2005, through day 181, 2005, was 314,424, giving an average of 1737 detections per processed day (181 days processed).

Events automatically located by the Spitsbergen array

During days 001, 2005, through 181, 2005, 19,024 local and regional events were located by the Spitsbergen array, based on automatic association of P- and S-type arrivals. This gives an average of 105.9 events per processed day (181 days processed). 72% of these events are within 300 km, and 89% of these events are within 1000 km.

U. Baadshaug

2.4 AS73 — Auxiliary Seismic Station at Jan Mayen

The IMS auxiliary seismic network includes a three-component station on the Norwegian island of Jan Mayen. The station location given in the protocol to the Comprehensive Nuclear-Test-Ban Treaty is 70.9˚N, 8.7˚W.

The University of Bergen has operated a seismic station at this location since 1970. A so-called Parent Network Station Assessment for AS73 was completed in April 2002. A vault at a new location (71.0^{o}N, 8.5^{o}W) was prepared in early 2003, after its location had been approved by the PrepCom. New equipment was installed in this vault in October 2003, as a cooperative

effort bertween NORSAR and the CTBTO/PTS. Continuous data from this station are being transmitted to the NDC at Kjeller via a satellite link installed in April 2000. Data are also made available to the University of Bergen.

J. Fyen

2.5 IS37 — Infrasound Station at Karasjok

The IMS infrasound network will include a station at Karasjok in northern Norway. The coordinates given for this station are 69.5˚N, 25.5˚E. These coordinates coincide with those of the primary seismic station PS28.

A site survey for this station was carried out during June/July 1998 as a cooperative effort between the Provisional Technical Secretariat of the CTBTO and NORSAR. The site survey led to a recommendation on the exact location of the infrasound station. The appropriate application forms have been sent to the local authorities to obtain the permissions needed to establish the station. Station installation is expected to take place in the year 2006, provided that adequate resources for further project planning and execution are made available.

S. Mykkeltveit

2.6 RN49 — Radionuclide Station on Spitsbergen

The IMS radionuclide network includes a station on the island of Spitsbergen. This station is also among those IMS radionuclide stations that will have a capability of monitoring for the presence of relevant noble gases upon entry into force of the CTBT.

A site survey for this station was carried out in August of 1999 by NORSAR, in cooperation with the Norwegian Radiation Protection Authority. The site survey report to the PTS contained a recommendation to establish this station at Platåberget, near Longyearbyen. The infrastructure for housing the station equipment was established in early 2001, and a noble gas detection system, based on the Swedish “SAUNA” design, was installed at this site in May 2001, as part of PrepCom’s noble gas experiment. A particulate station (“ARAME” design) was installed at the same location in September 2001. A certification visit to the station took place in October 2002, and the particulate station was certified on 10 June 2003. The equipment at RN49 is being maintained and operated in accordance with a contract with the CTBTO/PTS.

S. Mykkeltveit

3 Contributing Regional Seismic Arrays

3.1 NORES

NORES has been out of operation since a thunderstorm destroyed the station electronics on 11 June 2002.

J. Torstveit

3.2 Hagfors (IMS Station AS101)

Data from the Hagfors array are made available continuously to NORSAR through a cooperative agreement with Swedish authorities.

The mission-capable data statistics were 99.996% as compared to 99.71% for the previous reporting period. The net instrument availability was 99.996%.

There were no outages of all instruments in the reporting period.

Monthly uptimes for the Hagfors on-line data recording task, taking into account all factors (field installations, transmissions line, data center operation) affecting this task were as follows:

		Mission Capable	Net instrument availability
January	:	99.993%	99.992
February	:	100%	100%
March	:	99.993%	99.993%
April	:	100%	100%
May	:	99.993%	99.993%
June	:	100%	100%

J. Torstveit

Hagfors Event Detection Operation

Hagfors array detections

The number of detections (phases) reported from day 001, 2005, through day 181, 2005, was 154,216, giving an average of 852 detections per processed day (181 days processed).

Events automatically located by the Hagfors array

During days 001, 2005, through 181, 2005, 3698 local and regional events were located by the Hagfors array, based on automatic association of P- and S-type arrivals. This gives an average of 20.4 events per processed day (181 days processed). 71% of these events are within 300 km, and 91% of these events are within 1000 km.

U. Baadshaug

3.3 FINES (IMS station PS17)

Data from the FINES array are made available continuously to NORSAR through a cooperative agreement with Finnish authorities.

The mission-capable data statistics were 100%, the same as for the previous reporting period. The net instrument availability was 99.915%.

Monthly uptimes for the FINES on-line data recording task, taking into account all factors (field installations, transmissions line, data center operation) affecting this task were as follows:

		Mission Capable	Net instrument availability
January	:	100%	100%
February	:	100%	100%
March	:	100%	100%
April	:	100%	99.994%
May	:	99.999%	99.996%
June	:	99.998%	99.496%

J. Torstveit

FINES Event Detection Operation

FINES detections

The number of detections (phases) reported during day 001, 2005, through day 181, 2005, was 67,789, giving an average of 375 detections per processed day (181 days processed).

Events automatically located by FINES

During days 001, 2005, through 181, 2005, 2514 local and regional events were located by FINES, based on automatic association of P- and S-type arrivals. This gives an average of 13.9 events per processed day (181 days processed). 79% of these events are within 300 km, and 88% of these events are within 1000 km.

U. Baadshaug

3.4 Regional Monitoring System Operation and Analysis

The Regional Monitoring System (RMS) was installed at NORSAR in December 1989 and has been operated at NORSAR from 1 January 1990 for automatic processing of data from ARCES and NORES. A second version of RMS that accepts data from an arbitrary number of arrays and single 3-component stations was installed at NORSAR in October 1991, and regular operation of the system comprising analysis of data from the 4 arrays ARCES, NORES, FINES and

GERES started on 15 October 1991. As opposed to the first version of RMS, the one in current operation also has the capability of locating events at teleseismic distances.

Data from the Apatity array was included on 14 December 1992, and from the Spitsbergen array on 12 January 1994. Detections from the Hagfors array were available to the analysts and could be added manually during analysis from 6 December 1994. After 2 February 1995, Hagfors detections were also used in the automatic phase association.

Since 24 April 1999, RMS has processed data from all the seven regional arrays ARCES, NORES, FINES, GERES (until January 2000), Apatity, Spitsbergen, and Hagfors. Starting 19 September 1999, waveforms and detections from the NORSAR array have also been available to the analyst.

Phase and event statistics

Table 3.5.1 gives a summary of phase detections and events declared by RMS. From top to bottom the table gives the total number of detections by the RMS, the number of detections that are associated with events automatically declared by the RMS, the number of detections that are not associated with any events, the number of events automatically declared by the RMS, and finally the total number of events worked on interactively (in accordance with criteria that vary over time; see below) and defined by the analyst.

New criteria for interactive event analysis were introduced from 1 January 1994. Since that date, only regional events in areas of special interest (e.g, Spitsbergen, since it is necessary to acquire new knowledge in this region) or other significant events (e.g, felt earthquakes and large industrial explosions) were thoroughly analyzed. Teleseismic events of special interest are also analyzed.

To further reduce the workload on the analysts and to focus on regional events in preparation for Gamma-data submission during GSETT-3, a new processing scheme was introduced on 2 February 1995. The GBF (Generalized Beamforming) program is used as a pre-processor to RMS, and only phases associated with selected events in northern Europe are considered in the automatic RMS phase association. All detections, however, are still available to the analysts and can be added manually during analysis.

	Jan 05	Feb 05	Mar 05	Apr 05	May 05	Jun 05	Total
Phase detections	162,944	130,738	165,138	132,073	122,762	134,846	848,501
- Associated phases	5,380	4,386	6,283	4,076	5,569	4,659	30,353
- Unassociated phases	157,564	126,352	158,855	127,997	117,193	130,187	818,148
Events automatically declared by RMS	1,225	968	1,245	758	885	811	5,892
No. of events defined by the analyst	56	76	91	63	98	65	449

Table 3.5.1. RMS phase detections and event summary 1 January - 30 June 2005.

U. Baadshaug

B. Paulsen

4 NDC and Field Activities

4.1 NDC Activitities

NORSAR functions as the Norwegian National Data Center (NDC) for CTBT verification. Six monitoring stations, comprising altogether 113 field sensors, will be located on Norwegian territory as part of the future IMS as described elsewhere in this report. The four seismic IMS stations are all in operation today, and all of them are currently providing data to the CTBTO on a regular basis. The radionuclide station at Spitsbergen was certified on 10 June 2003, whereas the infrasound station in northern Norway will need to be established within the next few years. Data recorded by the Norwegian stations is being transmitted in real time to the Norwegian NDC, and provided to the IDC through the Global Communications Infrastructure (GCI). Norway is connected to the GCI with a frame relay link to Vienna.

Operating the Norwegian IMS stations continues to require increased resources and additional personnel both at the NDC and in the field. The PTS has established new and strictly defined procedures as well as increased emphasis on regularity of data recording and timely data transmission to the IDC in Vienna. This has led to increased reporting activities and implementation of new procedures for the NDC operators. The NDC carries out all the technical tasks required in support of Norway's treaty obligations. NORSAR will also carry out assessments of events of special interest, and advise the Norwegian authorities in technical matters relating to treaty compliance.

Verification functions; information received from the IDC

After the CTBT enters into force, the IDC will provide data for a large number of events each day, but will not assess whether any of them are likely to be nuclear explosions. Such assessments will be the task of the States Parties, and it is important to develop the necessary national expertise in the participating countries. An important task for the Norwegian NDC will thus be to make independent assessments of events of particular interest to Norway, and to communicate the results of these analyses to the Norwegian Ministry of Foreign Affairs.

Monitoring the Arctic region

Norway will have monitoring stations of key importance for covering the Arctic, including Novaya Zemlya, and Norwegian experts have a unique competence in assessing events in this region. On several occasions in the past, seismic events near Novaya Zemlya have caused political concern, and NORSAR specialists have contributed to clarifying these issues.

International cooperation

After entry into force of the treaty, a number of countries are expected to establish national expertise to contribute to the treaty verification on a global basis. Norwegian experts have been in contact with experts from several countries with the aim of establishing bilateral or multilateral cooperation in this field. One interesting possibility for the future is to establish NORSAR as a regional center for European cooperation in the CTBT verification activities.

NORSAR event processing

The automatic routine processing of NORSAR events as described in NORSAR Sci. Rep. No. 2-93/94, has been running satisfactorily. The analyst tools for reviewing and updating the solutions have been continually modified to simplify operations and improve results. NORSAR is currently applying teleseismic detection and event processing using the large-aperture NORSAR array as well as regional monitoring using the network of small-aperture arrays in Fennoscandia and adjacent areas.

Communication topology

Norway has implemented an independent subnetwork, which connects the IMS stations AS72, AS73, PS28, and RN49 operated by NORSAR to the GCI at NOR_NDC. A contract has been concluded and VSAT antennas have been installed at each station in the network. Under the same contract, VSAT antennas for 6 of the PS27 subarrays have been installed for intra-array communication. The seventh subarray is connected to the central recording facility via a leased land line. The central recording facility for PS27 is connected directly to the GCI (Basic Topology). All the VSAT communication is functioning satisfactorily. As of 10 June 2005, AS72 and RN49 are connected to NOR_NDC through a VPN link.

Jan Fyen

4.2 Status Report: Provision of data from Norwegian seismic IMS stations to the IDC

Introduction

This contribution is a report for the period January - June 2005 on activities associated with provision of data from Norwegian seismic IMS stations to the International Data Centre (IDC) in Vienna. This report represents an update of contributions that can be found in previous editions of NORSAR's Semiannual Technical Summary. It is noted that as of 30 June 2005, two of the Norwegian seismic stations providing data to the IDC have been formally certified.

Norwegian IMS stations and communications arrangements

During the reporting interval 1 January - 30 June 2005, Norway has provided data to the IDC from the four seismic stations shown in Fig. 4.2.1. PS27 —NOA) is a 60 km aperture teleseismic array, comprised of 7 subarrays, each containing six vertical short period sensors and a three-component broadband instrument. PS28 — ARCES is a 25-element regional array with an aperture of 3 km, whereas the Spitsbergen array (station code SPITS) has 9 elements within a 1-km aperture. AS73 — JMIC has a single three-component broadband instrument.

The intra-array communication for NOA utilizes a land line for subarray NC6 and VSAT links based on TDMA technology for the other 6 subarrays. The central recording facility for NOA is located at the Norwegian National Data Center (NOR_NDC).

Continuous ARCES data are transmitted from the ARCES site to NOR_NDC using a 64 kbits/s VSAT satellite link, based on BOD technology.

Continuous SPITS data has been transmitted to NOR_NDC via a VSAT terminal located at Platåberget in Longyearbyen (which is the site of the IMS radionuclide monitoring station

RN49 installed during 2001) up to 10 June 2005. The central recording equipment for the SPITS array has been moved to the University of Spitsbergen (UNIS). A 512 hps SHDSL link has been established between UNIS and NOR_NDC. Both AS72 and RN49 data are now transmitted to NOR_NDC over this link using VPN technology.

A minimum of seven-day station buffers have been established at the ARCES and SPITS sites and at all NOA subarray sites, as well as at NOR_NDC for ARCES, SPITS and NOA.

The NOA and ARCES arrays are primary stations in the IMS network, which implies that data from these stations is transmitted continuously to the receiving international data center. Since October 1999, this data has been transmitted (from NOR_NDC) via the Global Communications Infrastructure (GCI) to the IDC in Vienna. The AS73 — JMIC array is an auxiliary station in the IMS, and the JMIC data have been available to the IDC throughout the reporting period on a request basis via use of the AutoDRM protocol (Kradolfer, 1993; Kradolfer, 1996). In addition, continuous data from all three arrays is transmitted to the US NDC.

Uptimes and data availability

Figs. 4.2.2 and 4.2.3 show the monthly uptimes for the Norwegian IMS primary stations ARCES and NOA, respectively, for the period 1 Januar - 30 June 2005, given as the hatched (taller) bars in these figures. These barplots reflect the percentage of the waveform data that is available in the NOR_NDC data archives for these two arrays. The downtimes inferred from these figures thus represent the cumulative effect of field equipment outages, station site to NOR_NDC communication outage, and NOR_NDC data acquisition outages.

Figs. 4.2.2 and 4.2.3 also give the data availability for these two stations as reported by the IDC in the IDC Station Status reports. The main reason for the discrepancies between the NOR_NDC and IDC data availabilities as observed from these figures is the difference in the ways the two data centers report data availability for arrays: Whereas NOR_NDC reports an array station to be up and available if at least one channel produces useful data, the IDC uses weights where the reported availability (capability) is based on the number of actually operating channels.

Use of the AutoDRM protocol

NOR_NDC's AutoDRM has been operational since November 1995 (Mykkeltveit & Baadshaug, 1996). The monthly number of requests by the IDC for JMIC data for the period January - June 2005 is shown in Fig. 4.2.4.

NDC automatic processing and data analysis

These tasks have proceeded in accordance with the descriptions given in Mykkeltveit and Baadshaug (1996). For the period January - June 2005, NOR_NDC derived information on 509 supplementary events in northern Europe and submitted this information to the Finnish NDC as the NOR_NDC contribution to the joint Nordic Supplementary (Gamma) Bulletin, which in turn is forwarded to the IDC. These events are plotted in Fig. 4.2.5.

Data access for the station NIL at Nilore, Pakistan

NOR_NDC continued to provide access to the seismic station NIL at Nilore, Pakistan, through a VSAT satellite link between NOR_NDC and Pakistan's NDC in Nilore.

Current developments and future plans

NOR_NDC is continuing the efforts towards improving and hardening all critical data acquisition and data forwarding hardware and software components, so as to meet the requirements related to operation of IMS stations.

The NOA array was formally certified by the PTS on 28 July 2000, and a contract with the PTS in Vienna currently provides partial funding for operation and maintenance of this station. The ARCES array was formally certified by the PTS on 8 November 2001, and a contract with the PTS is in place which also provides for partial funding of the operation and maintenance of this station. Provided that adequate funding continues to be made available (from the PTS and the Norwegian Ministry of Foreign Affairs), we envisage continuing the provision of data from all Norwegian seismic IMS stations without interruption to the IDC in Vienna.

U. Baadshaug
S. Mykkeltveit
J. Fyen

References

Kradolfer, U. (1993): Automating the exchange of earthquake information. *EOS, Trans., AGU*, 74, 442.

Kradolfer, U. (1996): AutoDRM — The first five years, *Seism. Res. Lett.*, 67, 4, 30-33.

Mykkeltveit, S. & U. Baadshaug (1996): Norway's NDC: Experience from the first eighteen months of the full-scale phase of GSETT-3. *Semiann. Tech. Summ., 1 October 1995 - 31 March 1996*, NORSAR Sci. Rep. No. 2-95/96, Kjeller, Norway.

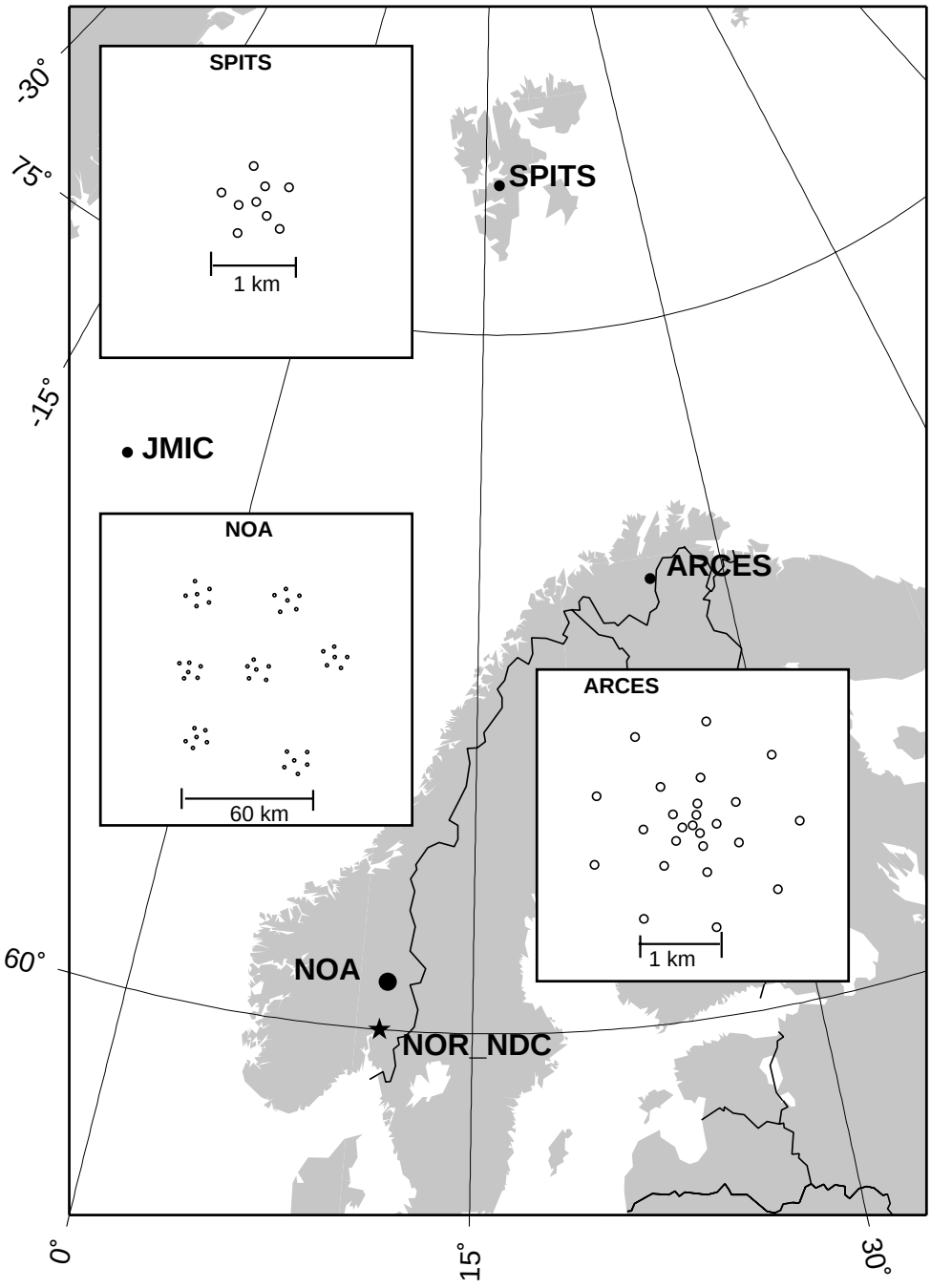

Fig. 4.2.1. The figure shows the locations and configurations of the three Norwegian seismic IMS array stations that provided data to the IDC during the period January - June 2005. The data from these stations are transmitted continuously and in real time to the Norwegian NDC (NOR_NDC). The stations NOA and ARCES are primary IMS stations, whereas JMIC is an auxiliary IMS station.

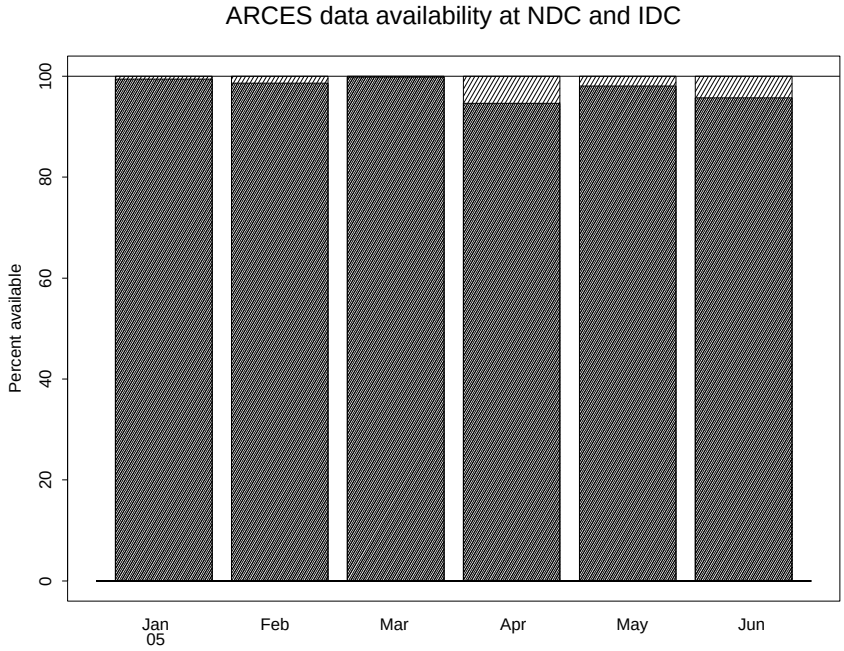

Fig. 4.2.2. The figure shows the monthly availability of ARCES array data for the period January - June 2005 at NOR_NDC and the IDC. See the text for explanation of differences in definition of the term "data availability" between the two centers. The higher values (hatched bars) represent the NOR_NDC data availability.

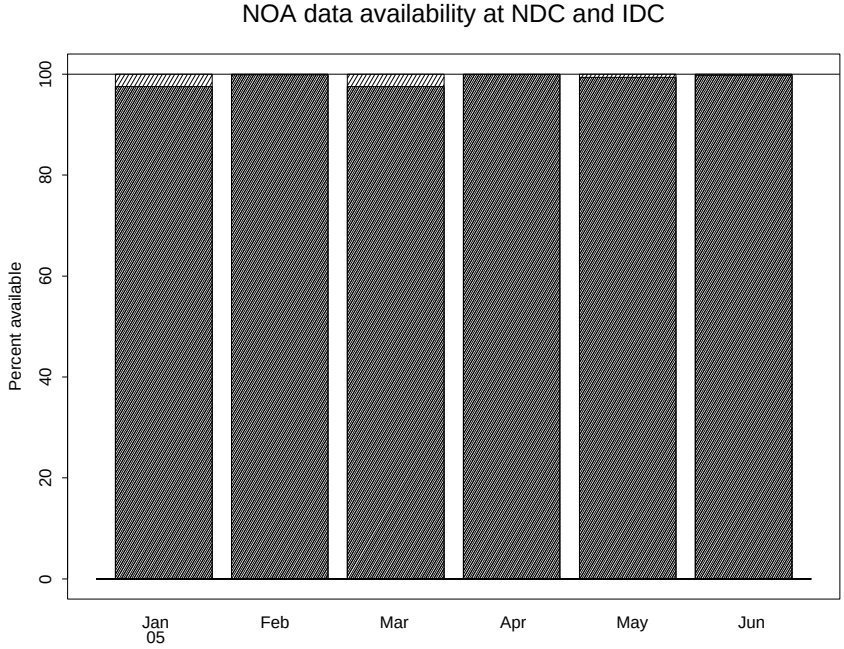

Fig. 4.2.3. The figure shows the monthly availability of NORSAR array data for the period January - June 2005 at NOR_NDC and the IDC. See the text for explanation of differences in definition of the term "data availability" between the two centers. The higher values (hatched bars) represent the NOR_NDC data availability.

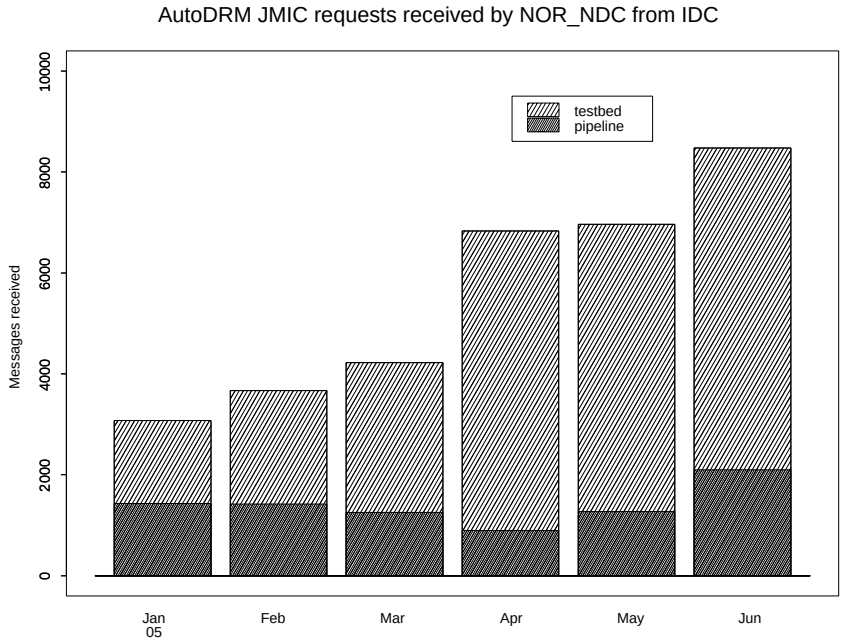

Fig. 4.2.4. The figure shows the monthly number of requests received by NOR_NDC from the IDC for JMIC waveform segments during January - June 2005.

Reviewed Supplementary events

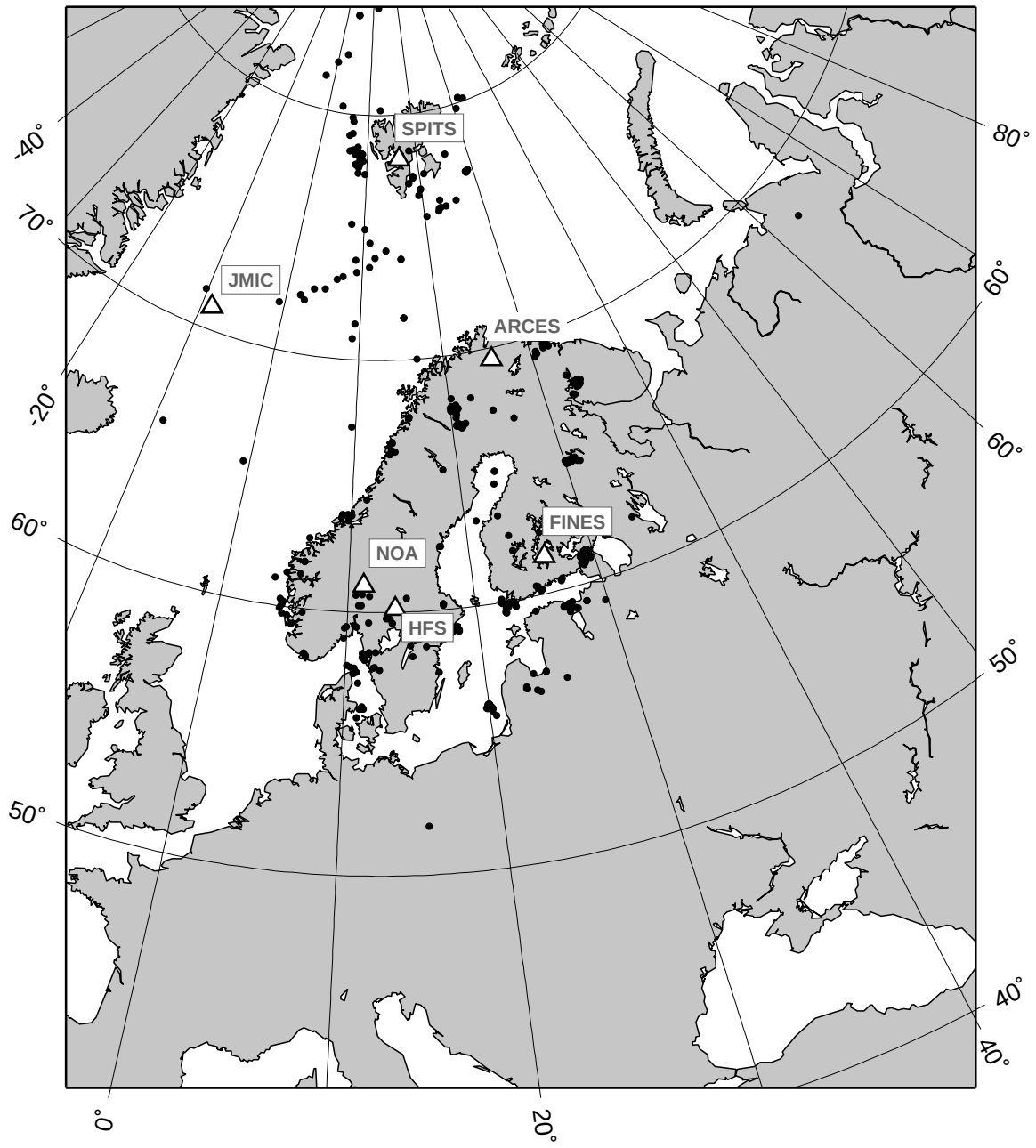

Fig. 4.2.5. The map shows the 509 events in and around Norway contributed by NOR_NDC during January - June 2005 as supplementary (Gamma) events to the IDC, as part of the Nordic supplementary data compiled by the Finnish NDC. The map also shows the seismic stations used in the data analysis to define these events.

4.3 Field Activities

The activities at the NORSAR Maintenance Center (NMC) at Hamar currently include work related to operation and maintenance of the following IMS seismic stations: the NOA teleseismic array (PS27), the ARCES array (PS28) and the Spitsbergen array (AS72). Some work has also been carried out in connection with the seismic station on Jan Mayen (AS73), the radionuclide station at Spitsbergen (RN49), and preparations for the infrasound station at Karasjok (IS37). NORSAR also acts as a consultant for the operation and maintenance of the Hagfors array in Sweden (AS101).

NORSAR carries out the field activities relating to IMS stations in a manner generally consistent with the requirements specified in the appropriate IMS Operational Manuals, which are currently being developed by Working Group B of the Preparatory Commission. For seismic stations these specifications are contained in the Operational Manual for Seismological Monitoring and the International Exchange of Seismological Data (CTBT/WGB/TL-11/2), currently available in a draft version.

All regular maintenance on the NORSAR field systems is conducted on a one-shift-per-day, five-day-per-week basis. The maintenance tasks include:

- Operating and maintaining the seismic sensors and the associated digitizers, authentication devices and other electronics components.
- Maintaining the power supply to the field sites as well as backup power supplies.
- Operating and maintaining the VSATs, the data acquisition systems and the intra-array data transmission systems.
- Assisting the NDC in evaluating the data quality and making the necessary changes in gain settings, frequency response and other operating characteristics as required.
- Carrying out preventive, routine and emergency maintenance to ensure that all field systems operate properly.
- Maintaining a computerized record of the utilization, status, and maintenance history of all site equipment.
- Providing appropriate security measures to protect against incidents such as intrusion, theft and vandalism at the field installations.

Details of the daily maintenance activities are kept locally. As part of its contract with CTBTO/PTS NORSAR submits, when applicable, problem reports, outage notification reports and equipment status reports. The contents of these reports and the circumstances under which they will be submitted are specified in the draft Operational Manual.

P.W. Larsen
K.A. Løken

4.4 Spitsbergen array refurbishment

As part of this contract, NORSAR has refurbished the Spitsbergen array to satisfy the IMS technical specifications. The refurbishment included upgrading 5 of the array sites to comprise three-component seismometers instead of the original vertical sensors. Both before and after this refurbishment, the Spitsbergen array configuration conforms to the minimum IMS requirement for a new seismic array, having 9 short-period vertical seismometers and one three-component broadband sensor.

As reported in NORSAR Sci. Rep. No. 1 and 2-2004, Guralp Systems was selected as the main vendor for the seismometers, digitizers and data acquisition system.See NORSAR Scientific Report No. 1-2005 for details of the refurbishment.

The station has provided 100% mission capable data availability throughout the reporting period.

The sensors at sites SPB3, SPB4 and SPB5 are all installed in sand. During a new expedition planned for August 2005, the remaining sensors will also be installed in sand. For the current flat acceleration response, the sensitivity for periods longer than 10 seconds may be too low to satisfy CTBTO requirements for a broadband sensor. This issue will be investigated further.

J. Fyen

5 Documentation Developed

Braun, T., J. Schweitzer, R.M. Azzara, D. Piccinni, M. Cocco & E. Boschi (2004): Results from the temporary installation of a small aperture seismic array in the Central Apennines and its merits for the local detection and location capabilities. Ann. di Geofisica, 47, 1557-1568.

Bungum, H. & O. Olesen (2005): The 31st August 1819 Lurøy earthquake revisited. Norw. J. Geology, in press.

Gibbons, S.J. & F. Ringdal (2005): Detecting the aftershock of the 16 August 1997 Kara Sea event by waveform correlation. **In:** Semiannual Technical Summary, 1 January - 30 June 2005, NORSAR Sci. Rep. 2-2005, Kjeller, Norway.

Gibbons, S.J. & F. Ringdal (2005): Automatic real-time detection and processing of regional seismic phases on the wide-aperture NORSAR array. **In:** Semiannual Technical Summary, 1 January - 30 June 2005, NORSAR Sci. Rep. 2-2005, Kjeller, Norway.

Levshin, A., C. Weidle & J. Schweitzer (2005): Surface wave tomography for the Barents Sea and surrounding regions. **In:** Semiannual Technical Summary, 1 January - 30 June 2005, NORSAR Sci. Rep. 2-2005, Kjeller, Norway.

Lindholm, C.D., M. Roth, H. Bungum & J.I. Faleide (2005): Probabilistic and deterministic seismic hazard results and influence of the sedimentary Møre Basin, NE Atlantic. Marine and Petroleum Geology, in press.

Maercklin, N., C. Haberland, T. Ryberg, M. Weber, Y. Bartov & DESERT Group (2004): Imaging the Dead Sea Transform with scattered seismic waves. Geophys. J. Int., 158(1), 179-186.

Molina, S. & C. Lindholm (2005): A logic tree extension of the capacity spectrum method developed to estimate seismic risk in Oslo. J. Earthq. Eng., in press.

Oye, V., H. Bungum & M. Roth (2005): Source parameters and scaling relations for mining related seismicity within the Pyhäsalmi ore mine, Finland. Bull. Seism. Soc. Am., in press.

Oye, V., A. Chavarria & P.E. Malin (2004): Determining SAFOD area microearthquake locations solely with Pilot Hole seismic array data. Geophys. Res. Lett., 31, L12S10, doi:10.1029/2003GL019403.

Ringdal, F. (2005): Semiannual Technical Summary, 1 July - 31 December 2004. NORSAR Sci. Rep. 1-2005, Kjeller, Norway, January 2005.

Ringdal, F. & J. Schweitzer (2005): Combined seismic/infrasonic processing: A case study of explosions in NW Russia. **In:** Semiannual Technical Summary, 1 January - 30 June 2005, NORSAR Sci. Rep. 2-2005, Kjeller, Norway.

6 Summary of Technical Reports / Papers Published

6.1 Detecting the aftershock of the 16 August 1997 Kara Sea event by waveform correlation

6.1.1 Introduction

On 16 August 1997, a small seismic disturbance occurred in the Kara Sea, approximately 100 km from the former Soviet nuclear test site on the island of Novaya Zemlya (see Figure 6.1.1). The event was recorded by several seismic stations and had an estimated magnitude m_b=3.5 (Ringdal et al., 1997). The close proximity of the event to the nuclear test site led to initial concerns that the event could have been a small clandestine nuclear explosion in violation of the Comprehensive Nuclear Test Ban Treaty (CTBT) which had been adopted by the United Nations eleven months previously. The event has been the subject of many subsequent publications (e.g. Richards and Kim, 1997; Hartse, 1998; Asming et al., 1998; Ringdal et al., 2002; Bowers et al., 2001; Kremenetskaya et al., 2001; Bowers, 2002; Schweitzer and Kennett, 2002) and the generally accepted conclusion, based upon location, spectral characteristics and other observations, is that the event was an offshore earthquake.

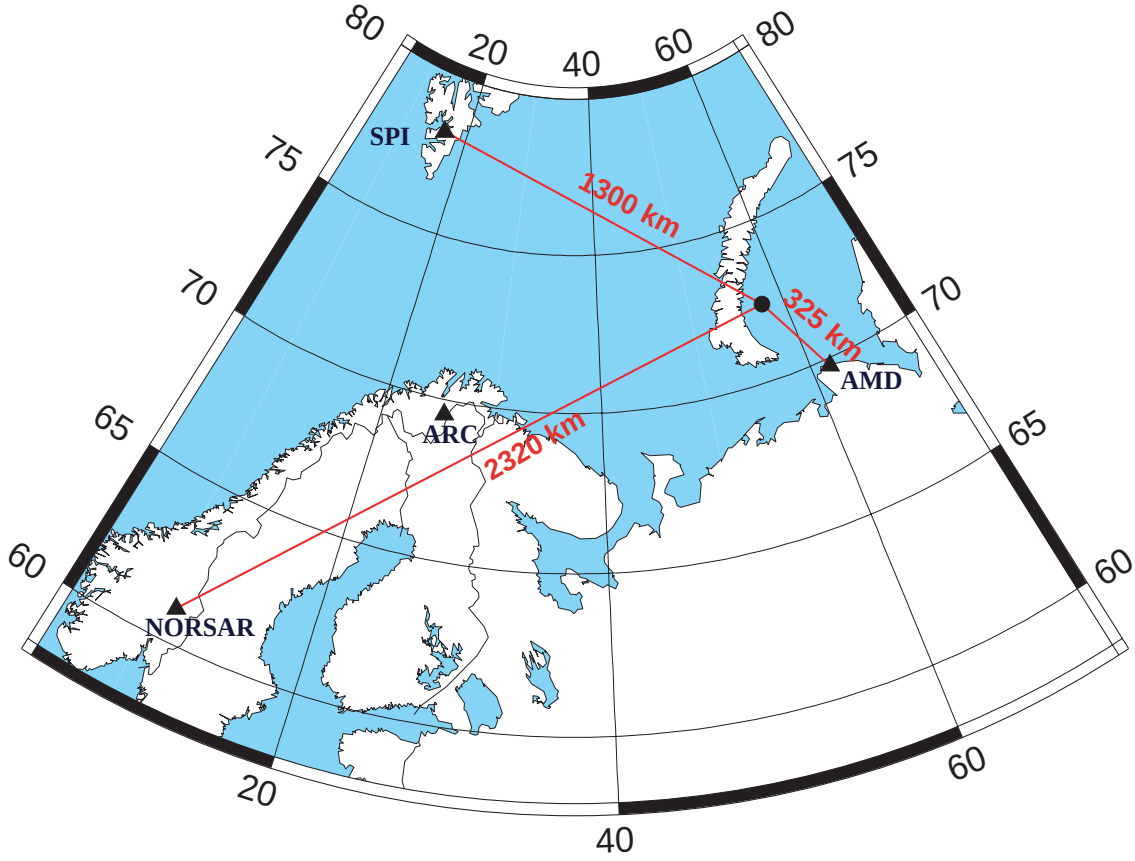

Fig. 6.1.1. Map indicating the location of the 16 August 1997 seismic disturbance in the vicinity of Novaya Zemlya. Also indicated are the locations of the SPITS and NORSAR seismometer arrays, the station at Amderma, Russia, and the ARCES array which was unusually and unfortunately not operational at the time of the event.

As Richards and Kim (1997) point out, one of the most compelling pieces of evidence for the classification of the event as an earthquake was the occurrence of a small event (assumed to be an aftershock) approximately four hours following the main event. Crucial to the classification of this second event as an approximately co-located aftershock is the similarity of the waveforms between the two events observed at the Amderma station in Russia at a distance of 325 km (Ringdal and Kremenetskaya, 1999; Ringdal et al., 2002), the only station to have recorded both events with a high signal-to-noise ratio (SNR). The Amderma waveforms for both events are displayed in Figure 6.1.2.

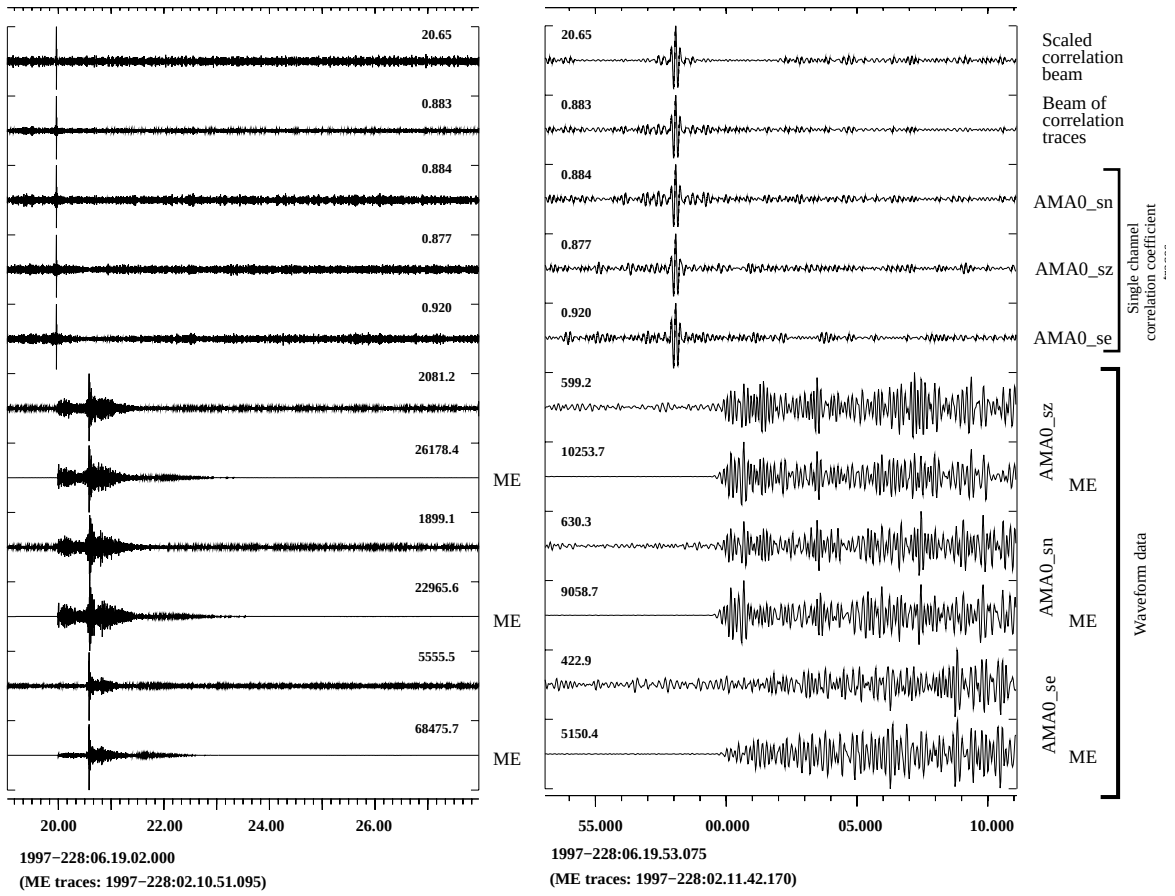

Fig. 6.1.2. The closest seismic station to record the event was the 4-site array at Amderma in Russia. The plots show the three components at the central AMA0 site. The traces labelled ME (master event) contain the signal from the main event and the remaining waveforms contain the signal from the presumed aftershock, aligned according to the time of maximum waveform-correlation. The correlation coefficient traces for the three components are displayed above the waveforms as labelled and the top two traces are the "beam" of the correlation traces and the rescaled beam (see Gibbons and Ringdal, 2005). All cross-correlation coefficients are obtained using data segments of length 60.0 seconds. The panel to the right is a close up of the P-arrival from the left panel. The waveform semblance between the two different events is clearest in these recordings given the high signal-to-noise-ratio (SNR) for both events. All waveforms bandpass filtered between 4.0 and 8.0 Hz.

The second event was of estimated magnitude m_b = 2.5 and was only detected by a single station of the International Monitoring System for the CTBT (IMS): the SPITS array on Spitsbergen at a distance of approximately 1300 km. Even at this station, only the P-arrival was detected and careful manual analysis was required for the identification of the signal. Given the

importance of this second event to the conclusions drawn about the nature of the source, it is a cause of some concern that it was only barely detected by the global seismic network designated to monitor signals from such events. (The station at Amderma is not part of the IMS.)

The correlation coefficient between waveforms from the main event and the aftershock recorded at Amderma, using a 60.0 second waveform template bandpass filtered between 4.0 and 8.0 Hz, was approximately 0.9 for all of the available data channels (Figure 6.1.2). The segment of the waveform taken from the master event begins at a time 1997-228:02.11.47.170 and the time of maximum correlation coefficient was 1997-228:06.19.58.075; these two times are separated by 14890.905 seconds. Subtracting the template waveform multiplied by 0.06551 from the aftershock waveform results in the smallest residual in the least squares sense; this gives a scaling factor of approximately 15 between the amplitudes for the two events.

The high degree of waveform semblance between the two events at the Amderma station indicates waveform correlation as a possible means of detecting signals at stations more distant from the event location. Gibbons and Ringdal (2004, 2005) have demonstrated the ability of waveform correlation (especially in the context of seismic arrays) to detect signals with SNR smaller than unity provided that a template signal exists from an event from a sufficiently close source location.

6.1.2 Detecting the Kara Sea event aftershock using waveform correlation on SPITS array data

The main event was detected with a high SNR for both P and S phases at the SPITS array (see the red-colored waveform in Figure 6.1.3). Waveforms from this master event were extracted and bandpass filtered between 4.0 and 8.0 Hz, a frequency band exhibiting a high SNR for this event. The filtered waveform was resampled to a frequency of 80 Hz and a 60.0 second long data segment was cut with a starting time of 02.13.44.915. Note that exactly the same time window was selected for all sensors of the array. The time-delays between the phase arrivals at the different sites do not constitute a problem; since we are attempting to detect another seismic event from the same source location, the sought signal will be associated with an identical time-delay at each of the receiver sites. Given the small aperture of the array, an incoming seismic wavefront will traverse all sites of the array within a second. The waveform template extracted was correlated with SPITS data over several hours both prior to and following the main event and a maximum of the array correlation coefficient beam was achieved at a time 1997-228:06.21.55.815, estimated using a spline interpolation of the discrete time series. The correlation results indicate that the origin time of the second event was 14890.9 seconds following the origin time of the main event.

The fully-normalised correlation coefficients for the single channels of the SPITS array are approximately 0.65. Although lower than the correlation coefficients observed for the data from Amderma, they are exceptionally high given the low SNR of the second event (blue traces in Figure 6.1.3). The peaks in the correlation coefficient traces are clearly visible for each of the individual channels; we conclude that the use of a seismic array was not actually necessary to able to detect this signal at SPITS using the signal from the first event as a template. However, it is important not to understate the importance of the observation that the correlation trace maxima occur simultaneously at each site. This observation provides evidence that the slowness vectors for phase arrivals from the two events are identical. A final observa-

tion from Figure 6.1.3 is that the arrival time of the P-phase from the second event can be estimated far more accurately given the presence of the master event waveform for comparison.

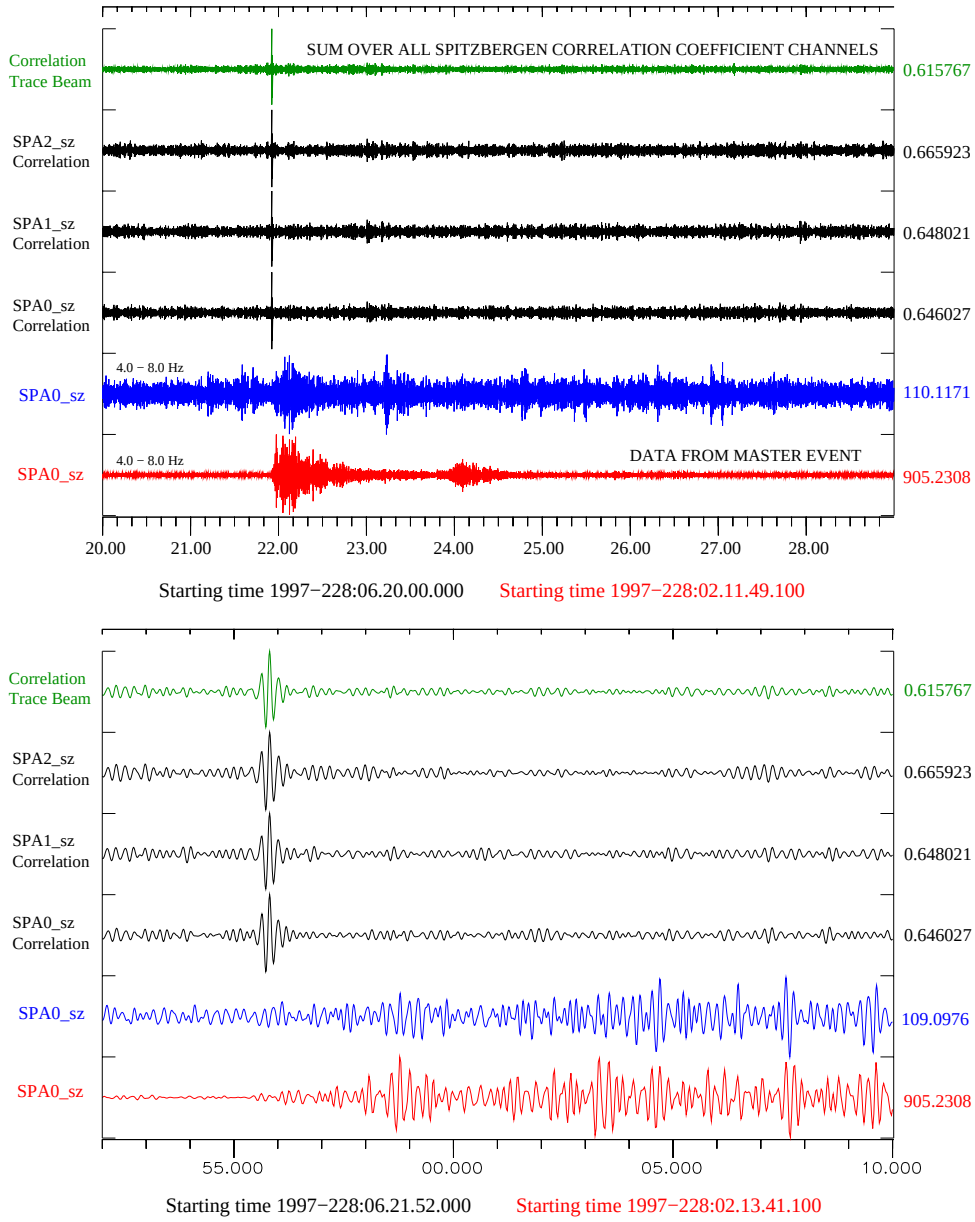

Fig. 6.1.3. Detection of an aftershock from the 16 August 1997 Kara Sea event using waveform correlation on the short period vertical channels of the Spitsbergen array. Each channel was bandpass filtered between 4.0 and 8.0 Hz and a 60 second long data segment was extracted from the master event signal (shown in red for SPA0 sz) with the first data segment beginning at 1997-228:02.13.44.913. The data containing the presumed aftershock was filtered in the same band (shown in blue for SPA0) and a trace of fully normalized correlation coefficients was calculated for each channel. The green channel is the summation of the 9 correlation coefficient traces. A clear peak is observed on the correlation beam at a time 1997-228:06.21.55.815. The lower panel is a zoom-in of the upper panel.

6.1.3 Detecting the Kara Sea event aftershock using waveform correlation on NORSAR array data

The closest IMS station to the site of the 16 August 1997 event was the regional array ARCES in the north of Norway. This station was unfortunately inoperational at the time of this event and, in such cases, every kind of observation possible from other (more distant) stations is potentially important. The large-aperture NORSAR array in the south of Norway is approximately 2300 km from the site of the Kara Sea event and recorded the main event with a reasonably high SNR. The signals are very different from those observed at the Spitsbergen array; the attenuation of energy at high frequencies means that the optimal SNR is obtained in a far lower frequency band: between approximately 2.5 and 5.0 Hz. It is noteworthy that, even at these somewhat lower frequencies, the waveforms from the various array sites are highly dissimilar.

Waveform data from the main event (recorded at the site NC602) is displayed in red in Figure 6.1.4 and the corresponding segment at the time of the aftershock is displayed above in blue. Given that these waveforms were filtered in approximately the optimal frequency band, it is quite evident that there is no chance of detecting the signal from the aftershock at NORSAR using a conventional energy detector. The data was filtered between 2.5 and 8.0 hz and data segments of length 60.0 seconds were extracted for each channel of the array using time-windows staggered to capture the initial P-arrival and the most energetic part of the signal for each site. These waveform segments were cross-correlated with filtered waveform data surrounding the time of the aftershock. Inspection of the single channel cross-correlation traces indicates no discernible peak values. However, a zero time-delay stacking of all of the available correlation channels results in an array correlation beam with a clear maximum at a time 1997-228:06.23.49.999: 14890.9 seconds following the reference time for the main event.

The signal from the second event is so weak at this distant station that it cannot be detected using a traditional energy detector. The signal to noise ratio is so low that cross-correlation using a single channel does not give a detection of the kind observed in Figure 6.1.3. However, beamforming of the correlation coefficient channels results in a spectacular array gain; local maxima of the single-channel correlation traces which result from coincidental similarity of unrelated seismic noise cancel out under the stacking operation, leaving only a superposition of the correlation maxima which result from the same deterministic waveform similarity. It is a remarkable result that such a detection is possible over a large aperture array where the waveforms themselves are largely incoherent. In traditional array processing, a requirement for array gain is incoherent noise and coherent signal. In contrast, array-based waveform correlation requires only incoherent noise in order to be applied successfully. The requirement for waveform coherency over the array is replaced by a requirement for coherency between the master waveform and the target waveform. The “signals” in this case are the cross correlation traces for each sensor, and the peaks of these traces occur simultaneously when the master event and the target event are co-located. Therefore, a zero-delay array beam of the correlation traces can be calculated without loss due to missteering or lack of signal coherence.

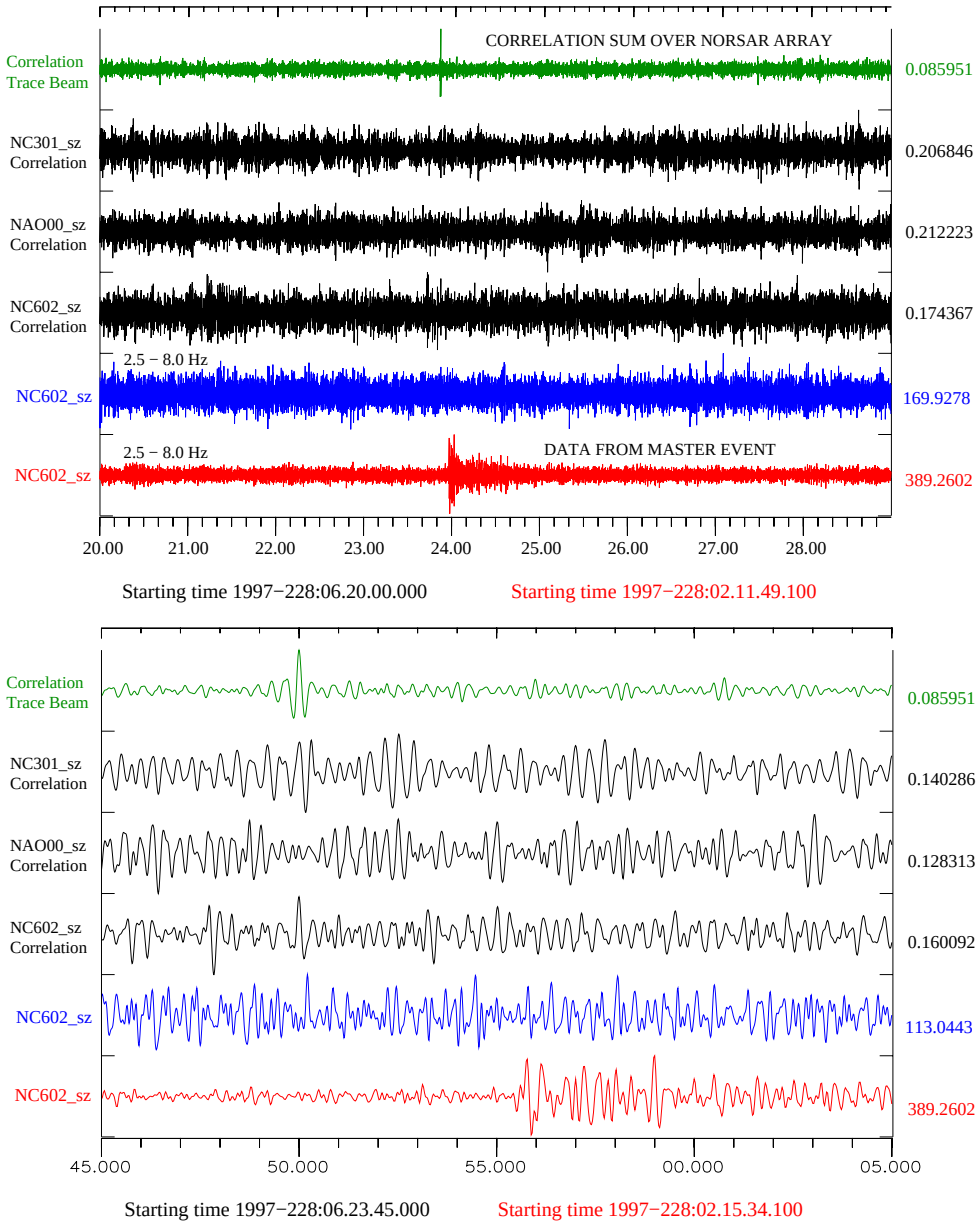

Fig. 6.1.4. Detection of the Kara Sea event aftershock by waveform correlation using the NORSAR array. The frequency band applied in this calculation is 2.5 - 8.0 Hz. The 60 second long time windows containing the master event signal are staggered by several seconds to account for the significant time delays across the array; the first master event time-window begins at 1997-228:02.15.39.087 for instrument NC301. The signal at this far more distant array is buried in the noise to a far greater extent than at SPI and in no filter band could this signal be detected with a conventional STA/LTA detector. While the SPI signal is very coherent over the array in the frequency band for which the SNR is optimal facilitating a reasonable SNR gain by conventional beamforming; this is not the case for the NOA signal. In contrast to the correlation displayed in Figure 3, the individual sensor correlation traces do not indicate clear simultaneous maxima. However, the beam (formed by applying the appropriate time-shifts to the individual correlation traces) displays a clear peak at time 1997-228:06.23.49.999.

6.1.4 Concluding remarks

We have examined waveforms from the main (m_b=3.5) Kara Sea event of 16 August 1997, and the m_b=2.5 event which occurred approximately 4 hours later, recorded at the Amderma station in Russia at a distance of approximately 325 km from the source location. At this station, the waveforms for both events exhibit a high SNR and a remarkable degree of waveform similarity between the two events. High correlation coefficients (~0.9) are obtained by correlating 60.0 second long data segments from the two events filtered between 4.0 and 8.0 Hz.

The detection of the second event using traditional array processing at the SPITS array (at a distance of approximately 1100 km) was marginal, resulting only in weak P-phase detections. We demonstrate that, using the signal from the main event as a waveform template, the second event is easily detected at SPITS using waveform correlation on a single seismometer channel. The correlation coefficients observed on the individual channels are approximately 0.65 for one minute long data segments (between 4 and 8 Hz) which is remarkably high considering the low SNR of the signal from the second event. Performing waveform correlation over the whole array provides us with the useful observation that the times of maximum cross-correlation are the same for each site which supports the claim that both signals come from approximately the same site.

The main event was also recorded by the large aperture NORSAR array at a distance of approximately 2300 km from the source; no detection by traditional processing is possible for the signal from the second event. Cross-correlating one minute long data segments from the main event with the corresponding waveforms from the time of the second event does not result in peaks on single-sensor correlation-traces which allow detection of the event. However, the event is clearly detectable on the NORSAR array by stacking the correlation coefficient traces from the various sites. This is a superb demonstration of how the cross-correlation functions are coherent across a large array or network even when the actual waveforms are not.

A time separation between the two events of approximately 14890.9 seconds was obtained from each of the three sites.

References

Asming, V. E., E. Kremenetskaya, and F. Ringdal (1998). Monitoring seismic events in the Barents/Kara Sea region, NORSAR Scientific Report: Semiannual Technical Summary No. 2 - 1997/1998. NORSAR, Kjeller, Norway. pp. 106-120.

Bowers, D. (2002). Was the 16 August 1997 Seismic Disturbance near Novaya Zemlya an Earthquake? Bull. seism. Soc. Am., 92, pp. 2400-2409.

Bowers, D., P. D. Marshall, and A. Douglas (2001). The level of deterrence provided by data from the SPITS seismometer array to possible violations of the Comprehensive Test Ban in the Novaya Zemlya region, *Geophys. J. Int.*, 146, pp. 425-438.

Gibbons, S. J. and F. Ringdal (2004). A waveform correlation procedure for detecting decoupled chemical explosions, NORSAR Scientific Report: Semiannual Technical Summary No. 2 - 2004. NORSAR, Kjeller, Norway. pp. 41-50.

Gibbons, S. J. and F. Ringdal (2005). The detection of rockbursts at the Barentsburg coal mine, Spitsbergen, using waveform correlation on SPITS array data, NORSAR Scientific Report: Semiannual Technical Summary No. 1 - 2005. NORSAR, Kjeller, Norway. pp. 35-48.

Hartse, H. E. (1998). The 16 August 1997 Novaya Zemlya Seismic Event as Viewed from GSN Stations KEV and KBS, Seism. Res. Lett., 69, pp. 206-215.

Richards, P. G. and W. Y. (1997). Testing the nuclear test-ban treaty, *Nature*, 389, pp. 781-782.

Ringdal, F., T. Kværna, E. Krementskaya, and V. Asming (1997). The seismic event near Novaya Zemlya on 16 August 1997, NORSAR Scientific Report: Semiannual Technical Summary No. 1 - 1997/1998. NORSAR, Kjeller, Norway. pp. 110-127.

Ringdal, F., E. Kremenetskaya, and V. Asming (2002). Observed characteristics of regional seismic phases and implications for P/S discrimination in the European Arctic, *Pure appl. geophys.*, 159, 701-719.

Schweitzer, J and B. L. N. Kennett (2002). Comparison of Location Procedures - The Kara Sea event of 16 August 1997, NORSAR Scientific Report: Semiannual Technical Summary No. 1 - 2002. NORSAR, Kjeller, Norway. pp. 97-103.

Steven J. Gibbons
Frode Ringdal

6.2 Automatic real-time detection and processing of regional seismic phases on the wide-aperture NORSAR array

6.2.1 Introduction

NORSAR has for a number of years carried out processing and analysis of seismic events in the European Arctic, using the regional array network in Fennoscandia and NW Russia. The regional processing system at the NORSAR Data Center comprises the following steps:

- Automatic single array processing, using a suite of bandpass filters in parallel and a beam deployment that covers both P and S type phases for the region of interest.
- An STA/LTA detector applied independently to each beam, with broadband f-k analysis for each detected phase in order to estimate azimuth and phase velocity.
- Single-array phase association for initial location of seismic events, and also for the purpose of chaining together phases belonging to the same event, so as to prepare for the subsequent multiarray processing.
- Multi-array event detection, using the Generalized Beamforming (GBF) approach (Ringdal and Kværna, 1989) to associate phases from all stations in the regional network
- Interactive analysis of selected events, resulting in a reviewed regional seismic bulletin, which includes hypocentral information, magnitudes and selected waveform plots.

Until recently, the large aperture NORSAR array in southern Norway has not been incorporated in this process, since a sufficiently reliable regional processing system has not been available for an array this size. The NORSAR array was designed in the late 1960s to detect low-yield underground nuclear explosions at teleseismic distances (Bungum et. al., 1971). The instruments, covering an aperture of approximately 100 km, were spaced to minimise the coherency of microseisms and thus provide an optimal SNR-gain for teleseismic signals between 0.5 and 2.0 Hz using classical beamforming with suitable steering parameters. After 1980, the focus in nuclear explosion monitoring turned towards the observation and interpretation of regional seismic phases and this motivated the development of the NORES regional seismic array and numerous subsequent arrays based upon this design (Mykkeltveit et. al., 1990). The GBF system provides fully automatic event locations by the association of phase detections made by the network of regional seismic arrays in Fennoscandia and Spitsbergen and the absence of detections from the NORES array (since June 2002) has led to a substantially worse detection and location capability for Southern and Western Norway.

A spatial reconfiguration of the NORSAR array to facilitate the processing of high-frequency regional phases using traditional regional array processing methods has been deemed undesirable because of the exciting possibilities which the large aperture NORSAR array represents in terms of detection of low-magnitude events using full waveform methods and because of the unique opportunity to study the variation of site effects over this large heterogeneous region. The vast majority of underground nuclear explosions occurred before the most of the regional arrays were built and the 35 year long database of high quality digital seismic data from the NORSAR array provides a unique and invaluble reference.

Traditional array processing methods are entirely inadequate to process high frequency regional phases over the NORSAR array due to the signal incoherence. The low attenuation in Fennoscandia means that many regional signals are best observed at high frequencies; signals

become incoherent over the NORSAR subarrays (aperture of the order 10 km) above approximately 3 Hz. It was noted many years ago by Ringdal et. al., 1972, however, that high frequency signals could be detected with a high SNR over the NORSAR array despite the incoherence of the actual waveforms by forming incoherent beams with the envelopes of filtered waveforms. Attempts to estimate propagation parameters from such a procedure have subsequently failed due to the very different time-histories recorded at the different sites. Gibbons, Kværna and Ringdal (2003) discuss further the issues associated with the detection and identification of regional phases over the large aperture array, and present an algorithm for the detection of regional phases at sub-array level using incoherent beams and a subsequent association of estimated onset picks. Whilst the method worked demonstrably well for certain events, the output was never included in the standard GBF system due to an unacceptable number of false alarms. The following section outlines a method of phase detection and parameter estimation based upon continuous spectral estimates which has proved to be remarkably robust and, although still in an experimental phase, contributes to the online GBF.

6.2.2 Phase detection and parameter estimation using continuous spectral estimates

The multitaper method of Thomson (1982) facilitates the calculation of low-variance estimates for the amplitude density spectrum, *A(f)*, over relatively short time windows and recent improvements in CPU power mean that it is now trivial to compute running "spectrograms" (i.e. *A(f)* as a continuous function of time) in real-time for the entire NORSAR array. In particular, the function

$$D(f,t) = \log_{10}(A(f)_{t+}) - \log_{10}(A(f)_{t-})$$

measures the ratio between the energy in a time-window immediately following time *t* and the energy in a time-window immediately prior to time *t*. Figure 6.2.1 shows the functions *A(f,t)* and *D(f,t)* for two channels of the NORSAR array for a regional event. The *D(f,t)* function reaches a maximum value in the vicinity of the phase arrival time with variation determined by how emergent the signal is and how the amplitude at each site varies with time. However, the form of the *D(f,t)* function is a far more stable indicator of the arrival of a phase than the SNR of a waveform filtered in a given frequency band. Under the traditional power detectors of the kind proposed by Freiburger (1963), frequency bands are chosen a priori and are not necessarily optimal for a given signal; the *D(f,t)* function only attains significant values for the frequencies at which an SNR is observed. A time window length of 3.0 seconds was deemed ideal for the identification of regional phases at NORSAR; the sought after phases generally have a frequency content between 2.0 and 16.0 Hz and this length of time window is generally sufficient to ensure that the maximum value comes close to the phase onset time even for quite emergent signals.

These functions of time and frequency can be beamformed in the same way as seismograms using the plane wave delays appropriate for regional phases. Although the NORSAR array is too large for the true validity of such propagation models, the deviations from plane waves generally cancel out under the beamforming process resulting in a maximum value which typically fits the arrival time at the NB200 central array element with a surprising consistency. Eventually, the plane-wave time delays employed during the current experimental phase will be replaced by calibrated time delays. The detection process is executed by calculating a scalar function of time which is a mean of *D(f,t)* in a frequency band appropriate for the aniticipated

phase. Following a detection reduction algorithm, the slowness of the detected phase is estimated by beamforming the differentiated spectrograms on a dense grid; the slowness results for the northern Norway event displayed in Figure 6.2.1 are shown in Figure 6.2.2. For each of the phases shown, the slowness estimate is close to that anticipated from the reviewed event location.

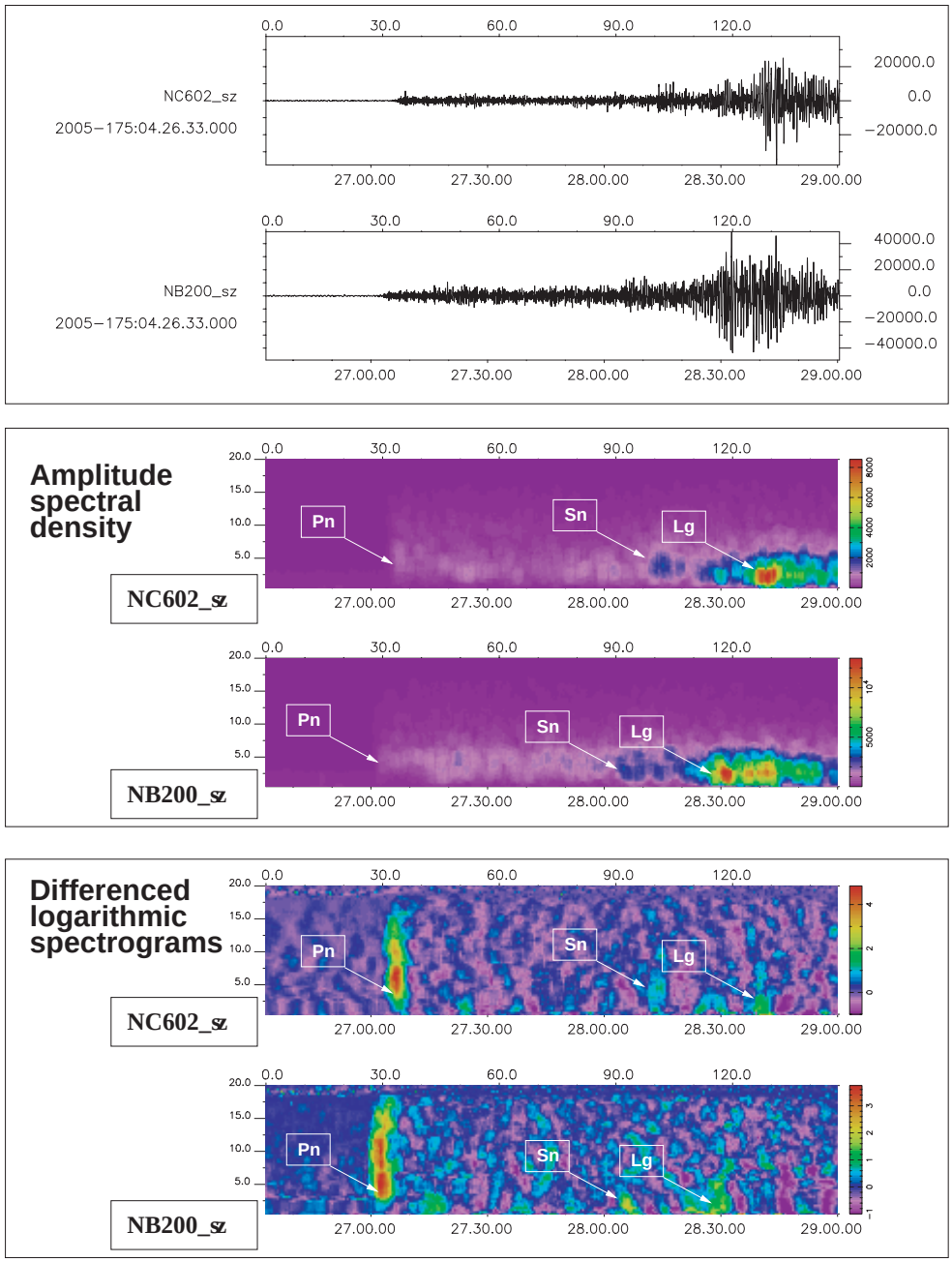

Fig. 6.2.1. Seismograms from two elements of the NORSAR array (top panel) for an earthquake in Northern Norway (distance approximately 610 km) with corresponding spectrograms, A(f,t), (center panel) and the function $D(f,t) = \log_{10}(A(f)_{t+}) - \log_{10}(A(f)_{t-})$ (lower panel). The secondary phases exhibit relatively poor spectral contrast on single channel spectrograms. This contrast is improved greatly by beamforming these functions using the appropriate delay times. The large number of array sites and large intersite distances mean that features which are not observed at a majority of sites at the appropriate times are rarely detected.

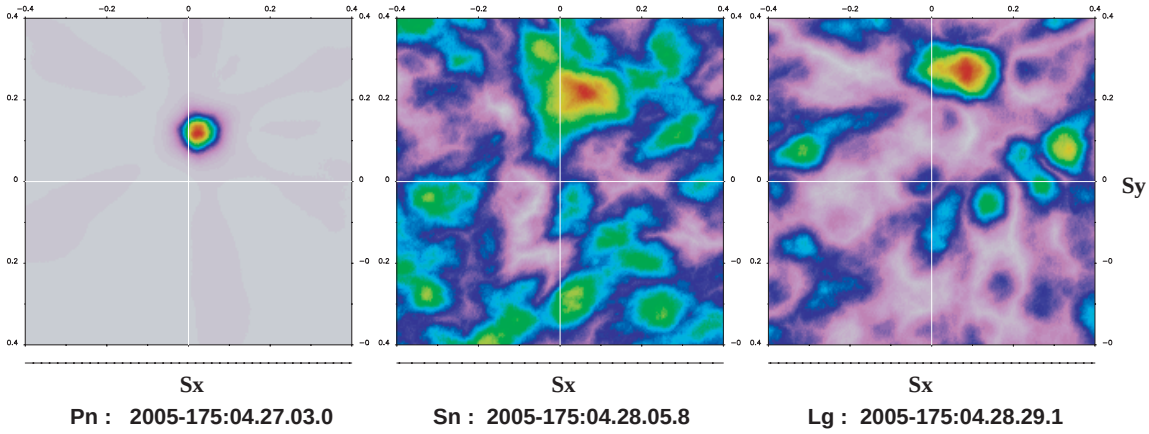

Fig. 6.2.2. Slowness estimates from the large aperture NORSAR array for the Pn, Sn, and Lg phases from the North Norway event on June 24th 2005 using spectrogram beamforming at the times indicated. The automatic location estimate incorporating these phase detections, together with detections from the regional arrays in Fennoscandia, is found on http://www.norsar.no/NDC/bulletins/gbf/2005/GBF05175.html

6.2.3 Inclusion of detections from the NORSAR array in the GBF automatic event location system

Detections from the NORSAR array have been incorporated in the GBF system since March 16, 2005, and, despite the unconventional method employed, have contributed significantly to the automatic detection capability in this region and have reduced considerably the analyst workload. Since operations began, an average of 40 detections per day have been registered for regional, far regional and some teleseismic events. Most teleseismic events are missed since the waveforms are bandpass filtered above 1.8 Hz; such signals are captured by the traditional processing of the NORSAR array. Although the number of detections made is far smaller than for the regional arrays, the large aperture of the array, combined with a conservative detection threshold, ensures that almost all detections are the result of genuine regional phases and the vast majority are subsequently associated with phases from the regional arrays.

Local Rg detections which can often dominate the detection lists from the other arrays are not made since such phases would not excite all seven subarrays at times consistent with regional body waves or Lg phases. Given that the energy contrast is so low for many coda phases, few are detected using this process; beamforming with the appropriate steering parameters on a coherent array is required to achieve a sufficient SNR for detection. This is regrettable in that the rich information available to a regional array is lost, but, for the multi-array phase association (GBF), the absence of many coda detections has meant that the NORSAR contributions have in many cases provided the best constraints on the solution since the detections made are almost inevitably the first P- and first S- phases at these sites.

Phase arrivals from weaker and more distant events than those currently detected can be observed using the spectrogram beamforming method. However, estimates of propagation parameters for these phases using spectrogram beampacking were frequently found to be spurious for the more marginal signals. The detection threshold has been set such that essentially all slowness estimates obtained are qualitatively correct, meaning that the azimuth error is small

and that the phase classification (P, Pn/Pg, Sn, Lg) is correctly assigned. A reduction in the detection threshold would greatly increase the number of detections, but the proportion of phase detections with qualitatively incorrect propagation parameter estimates would increase dramatically. Conisderable research is required in order to characterise the spectral shapes which can be anticipated from low amplitude phases and to design algorithms which can estimate robustly slowness and azimuth. It may be that a source-specific spectrogram correlation algorithm (analogous to the waveform correlation detection and location algorithm of Withers et al., 1999) is the best procedure.

6.2.4 Concluding remarks

We have implemented a new, experimental, processing system for incorporating regional seismic phases detected by the large NORSAR (NOA) array into the Generalized Beamforming process currently in use at NORSAR for on-line automatic detection and location of seismic events in the European Arctic. The system represents a significant improvement over previous processing systems for large arrays, and we recommend that this method be further developed for improving automatic detection and location using local or regional networks.

References

Bungum, H., E. S. Husebye and F. Ringdal (1971). The NORSAR array and preliminary results of data analysis, *Geophys. J. R. Astr. Soc., 25*, 115-126.

Freiburger, W. F.(1963). An approximation method in signal detection, *Quart. J. App. Math.*, 20, 373--378.

Gibbons, S. J., Kværna, T. and Ringdal, F. (2003). Processing of regional phases using the large aperture NOA array, Semiannual Technical Summary, 1 January - 30 June 2003, NORSAR Sci. Rep. 2-2003, Norway. pp 62-76.

Mykkeltveit, S., F. Ringdal, T. Kværna and R. W. Alewine (1990). Application of regional arrays in seismic verification research, *Bull. Seism. Soc. Am., 80*, 1777-1800.

Ringdal, F. and T. Kværna (1989). A multichannel processing approach to real time network detection, phase association and threshold monitoring, Bull. Seism. Soc. Am., 79, 1927-1940.

Ringdal, F., E. S. Husebye and A. Dahle (1972). Event detection problems using a partially coherent seismic array, NORSAR Tech. Rep. 45, Kjeller, Norway.

Thomson, D. J. (1982). Spectrum Estimation and Harmonic Analysis, Proc. IEEE, 70 , 1055--1096.

Withers, M., R. Aster, and C. Young (1999). An Automatic Local and Regional Seismic Event Detection and Location System Using Waveform Correlation, *Bull. Seism. Soc. Am., 89*, 657-669.

Steven J. Gibbons
Frode Ringdal

6.3 Surface Wave Tomography for the Barents Sea and Surrounding Regions

6.3.1 Introduction

Existing global and regional tomographic models have limited resolution in the European Arctic due to the small number of seismic stations, relatively low regional seismicity, and limited knowledge of the crustal structure. During the last decades, new seismic stations were permanently or temporarily installed in and around this region. However, many of the data from these stations are not easily accessible via the international data centers but only by direct request to the different data operators.

Recently, a new crustal model of the Barents Sea and the surrounding areas had been derived in a joint project of the University of Oslo, NORSAR and the USGS (Bungum *et al.*, 2004; 2005). This model, with its detailed information on crustal thickness and sedimentary basins in the area, is a valuable constraint for the tomographic inversion of the upper mantle velocity structure based on surface wave data.

6.3.2 Data collection

In this project, we have extensively searched for long period and broadband data observed at the seismic stations and arrays in the area from the beginning of the 1970s until 2005. We were able to retrieve surface wave observations from the data archives at NORSAR, University of Bergen, the Kola Science Center in Apatity, the Geological Service of Denmark and the University of Helsinki, in addition to the data, retrieved from the international data centers IRIS and GEOFON. The full list of used stations is given in Table 6.3.1 and a map with the positions of the stations is shown on top of Fig. 6.3.1.

In these data archives, not yet analyzed Love- and Rayleigh-wave data were identified and for more than 150 seismic events (earthquakes and nuclear explosions) dispersion curves were measured. The list of these events is presented in the Table 6.3.2 and the map on bottom of Fig. 6.3.1 shows the geographic distribution of the events.

6.3.3 Data analysis

From the surface wave recordings, group velocities of Love and Rayleigh waves were measured in the period range between10 and150 s using the program package for Frequency-Time Analysis developed at the University of Colorado (Ritzwoller & Levshin, 1998). After several cleaning procedures (Ritzwoller & Levshin, 1998), the new measurements were combined with the existing set of group velocity measurements provided by the Center for Imaging the Earth's Interior at the Colorado University (CU; see Levshin *et al.*, 2001). From this CU data set only those paths were selected, which were completely inside the cell [50 – 90° N, 60° W – 160° E], such that the entire data set consists of paths within the same regional frame. From cluster analysis (Ritzwoller & Levshin, 1998) of the root-mean-square of the group velocity measurements for the new data set in the considered period range was estimated as 0.010 – 0.015 km/s for Rayleigh waves and 0.015 – 0.025 km/s for Love waves.

To demonstrate the amount of new surface wave observations, we compare in Fig. 6.3.2 the number of newly analyzed Love and Rayleigh waves with the number in the preselected CU

data set. Obviously, the new data set increased the ray density and consequently the resolution of the planned tomography. In particular for shorter periods, the number of rays crossing the target area was increased by more than 200% for Rayleigh waves and close to 200% for Love waves. For longer periods (*i.e.*, T > 80 s), the ratio of added data significantly drops since large seismic events, necessary to generate long period radiation, are very rare in this region.

6.3.4 2D-inversion for group velocity tomographic maps

A tomographic inversion for two-dimensional group-velocity maps has been done for a set of periods between 14 and 90 s following the procedure by Barmin *et al.*, 2001. In all cases, we inverted the combined data set of the newly acquired and analyzed data and the preselected CU data. As first results, we present in Figs. 6.3.3, 6.3.4, and 6.3.5 the resulting group-velocity maps for Love and Rayleigh waves at three different periods: 16, 25, and 40 s, respectively.

To illustrate the newly achieved, high path density, we also present in Figs. 6.3.3, 6.3.4, and 6.3.5 all ray paths of the newly acquired data for both, Love and Rayleigh waves on top of the figures. In the middle of the figures, we show these ray paths again but with all rays paths of the preselected CU data set on top. Note the many gaps in the preselected CU data set, for which group velocity information is now available.

The Love and Rayleigh group-velocity maps are shown at the bottom of Figs. 6.3.3, 6.3.4, and 6.3.5. The group-velocity maps derived from the combined data set, show the lateral deviation of the group velocities from the average velocity in percent. Note that these deviations are up to ±36% for Love and Rayleigh waves with a period of 16 s. This reflects the strong lateral heterogeneity of the Earth's crust in this region, which changes between the mid-oceanic ridge system (white line on the map), thick sedimentary basins in the Barents Sea, and old continental shields.

Sensitivity kernels for Love waves and Rayleigh waves are different; Rayleigh waves are sensitive for deeper structures than Love waves with the same signal period. Therefore, jointly analyzing the crustal structure with both Love and Rayleigh waves gives additional confirmation for an inverted velocity model. Note, *e.g.*, that the geographical pattern of group-velocity variations for Love waves at a period of 25 s (Fig. 6.3.4, on the right at the bottom) is similar to the pattern of group-velocity variations for Rayleigh waves at a period of 16 s (Fig. 6.3.3, on the left at the bottom). A similar relation is between the 40 s Love waves and the 25 s Rayleigh waves.

6.3.5 Further work: 3D-inversion for the shear velocity structure

The planned next step will be an inversion of all group-velocity maps (Love and Rayleigh waves) into a 3D shear-velocity model for the whole region (Shapiro & Ritzwoller, 2002). As additional constraints for thew inversion the thickness of the sedimentary layers and the Moho depth, as they were derived by Bungum *et al.* (2004; 2005) will be included. The result should yield a new, robust 3D model of the velocities in the upper mantle beneath the greater Barents Sea region down to about 250 km.

Acknowledgements

For this study we requested and retrieved broadband and long periodic data from the Norwegian National Seismic Network (NNSN, University in Bergen), Kola Regional Seismological Center (KRSC, Apatity), Danmarks og Grønlands Geologiske Undersøgelse (GEUS, Copenhagen), Totalförsvarets forskningsinstitut (FOI, Stockholm), British Geological Service (BGS, Edinburgh), the Finish National Seismic Network (FNSN, University of Helsinki), and the international network operators and data centers IRIS and GEOFON. That they all made their data available for this study is gratefully acknowledged.

Anatol Levshin, University of Colorado
Christian Weidle, University of Oslo
Johannes Schweitzer

References

Barmin, M. P., M. H. Ritzwoller & A. L. Levshin (2001). A fast and reliable method for surface wave tomography, *Pure Appl. Geophys.*, **158**, 1351-1375.

Bungum, H., O. Ritzmann, N. Maercklin, J. I. Faleide, W. D. Mooney & S. T. Detweiler (2005). Three-dimensional model for the crust and upper mantle in the Barents Sea region, *Eos. Trans. Am Geophys. Union*, **86**, 160-161.

Bungum, H., O. Ritzmann, J. I. Faleide, N. Maercklin, J. Schweitzer, W. D. Mooney, S. T. Detweiler & W. S. Leith (2004). Development of a three-dimensional velocity model for the crust and upper mantle in the Barents Sea, Novaya Zemlya and Kola-Karelia regions, in *Proceedings of the 26th Seismic Research Review: Trends in Nuclear Explosion Monitoring*, Orlando, FL (September 21 – 23, 2004).

Levshin, A. L., M. H. Ritzwoller, M. P. Barmin, A. Villaseñor & C. A. Padgett (2001). New constraints on the arctic crust and uppermost mantle: surface wave group velocities, P_n, and S_n, *Phys. Earth Planet. Int.*, **123**, 185-204.

Ritzwoller, M. H. & A. L. Levshin (1998). Eurasian surface wave tomography: Group velocities, *J. Geophys. Res.*, **103**, 4839-4878.

Shapiro, N. M. & M. H. Ritzwoller (2002). Monte-Carlo inversion for a global shear velocity model of the crust and upper mantle, *Geophys. J. Int.*, **151**, 88-105.

Table 6.3.1. List of seismic stations from which surface-wave data could be retrieved to increase the ray coverage in the Barents Sea and surrounding regions (see also Fig. 6.3.1). The abbreviations in the network-affiliation column stand for: AWI – Alfred-Wegener-Institute for Polar and Marine Research, BGS – British Geological Service, CNSN – Canadian National Seismograph Network, FNSN – Finish National Network (University in Helsinki), FOI – Totalförsvarets forskningsinstitut (Sweden), GEUS - Danmarks og Grønlands Geologiske Undersøgelse, GRSN – German Regional Seismic Network, IDA – International Deployment of Accelerometers, IMS – International Monitoring System, IRIS – Incorporated Research Institutions for Seismology, KRSC – Kola Regional Seismological Center, MASI99 – Temporal net of seismic stations in Finmark operated by NORSAR and the University of Potsdam (Germany), NNSN – Norwegian National Seismic Network (University in Bergen), RUB – Ruhr University Bochum, UK – University of Kiel, and USGS – US Geological Survey. The data availability for some of the stations may be longer than known to us.

Station	Latitude	Longitude	Location	Network Affiliation	LP or BB Data Availability
AMD	69.7420	61.6550	Amderma	KRSC	08.1998 -12.2003
APZ9	67.5686	33.4050	Apatity	KRSC	09.1992 -
ARE0	69.5349	25.5058	ARCES Array	NORSAR/IMS	09.1987 -
ARU	56.4302	58.5625	Arti	IRIS/IDA/IMS	09.1989 -
BER	60.3870	5.3348	Bergen	NNSN	01.2004 -
BILL	68.0651	166.4524	Bilibino	IRIS/USGS/IMS	08.1995 -
BJO1	74.5023	18.9988	Bjørn Øya (Bear Island)	NNSN	06.1996 -
BORG	64.7474	-21.3268	Borgarnes	IRIS/IDA	07.1994 -
BSD	55.1139	14.9147	Bornholm	GEUS	01.1996 -
COP	55.6853	12.4325	København	GEUS	09.1999 -
DAG	76.7713	-18.6550	Danmarkshavn	GEUS/GEOFON/AMI	06.1998 -
DSB	53.2452	-6.3762	Dublin	GEOFON	12.1993 -
EDI	55.9233	-3.1861	Edinburgh	BGS	06.1996 -
ESK	55.3167	-3.2050	Eskdalemuir	IRIS/IDA/BGS	09.1978 -
FIA1	61.4444	26.0793	FINES Array	FNSN/IMS	04.2001 -
HFC2	60.1335	13.6945	Hagfors Array	FOI/IMS	08.2001 -
HFSC2	60.1326	13.6958	Hagfors Array (closed)	FOI	01.1992 - 09.2003
HLG	54.1847	7.8839	Helgoland	UK/GEOFON	12.2001 -
IBBN	52.3072	7.7566	Ibbenbüren	RUB/GEOFON/GRSN	07.1999 -
JMI	70.9283	-8.7308	Jan Mayen (closed)	NNSN	10.1994 - 04.2004
JMIC	70.9866	-8.5057	Jan Mayen	NORSAR/IMS	10.2003 -
KBS	78.9256	11.9417	Ny-Ålesund	NNSN/AWI/GEOFON/ IRIS/USGS	10.1986 - 09.1987 11.1994 -
KEV	69.7553	27.0067	Kevo	FNSN/IRIS/USGS	10.1981 -
KIEV	50.6944	29.2083	Kiev	IRIS/USGS	01.1995 -
KONO	59.6491	9.5982	Kongsberg	NNSN/IRIS/USGS	09.1978 -
KWP	49.6305	22.7078	Kalwaria Paclawska	GEOFON	06.1999 -
LID	54.5481	13.3664	Liddow	GRSN/GEOFON	01.1994 - 11.1995
LRW	60.1360	-1.1779	Lerwick	BGS	08.2003 -
LVZ	67.8979	34.6514	Lovozero	IRIS/IDA	10.1992 -
MA00	69.5346	25.5056	at ARCES A0	MASI99	08.1999 - 10.1999
MA01	69.3752	24.2122	Suosjavrre	MASI99	05.1999 - 10.1999
MA02	69.1875	25.7033	Kleppe	MASI99	05.1999 - 10.1999
MA03	70.0210	27.3962	Sirma	MASI99	05.1999 - 10.1999
MA04	69.7127	29.5058	Neiden	MASI99	05.1999 - 10.1999
MA05	69.4533	30.0391	Svanvik	MASI99	05.1999 - 08.1999
MA06	70.4813	25.0609	Russenes	MASI99	05.1999 - 10.1999
MA07	69.7050	23.8203	Sautso	MASI99	05.1999 - 10.1999
MA08	70.1278	23.3736	Leirbotn	MASI99	05.1999 - 10.1999
MA09	69.4566	21.5333	Reisadalen	MASI99	05.1999 - 10.1999
MA10	69.5875	23.5273	Suolovuobme	MASI99	05.1999 - 10.1999

Station	Latitude	Longitude	Location	Network Affiliation	LP or BB Data Availability
MA11	68.6595	23.3219	Kivilompolo	MASI99	05.1999 - 10.1999
MA12	69.8349	25.0823	Skoganvarre	MASI99	05.1999 - 10.1999
MA13	70.3161	25.5155	Børselv	MASI99	05.1999 - 10.1999
MBC	76.2417	-119.3600	Mould Bay	CNSN/IMS	04.1994 -
MHV	54.9595	37.7664	Michnevo	GEOFON	05.1995 -
MOL	62.5699	7.5470	Molde	NNSN	11.2000 - 05.2001
MOR8	66.2852	14.7316	Mo i Rana	NNSN	05.2001 - 08.2002
MORC	49.7766	17.5428	Moravsky Beroun	GEOFON	11.1993 -
MUD	56.4559	9.1733	Mønsted	GEUS	12.1999 -
N1002	60.4438	10.3690	NORSAR Array	NORSAR	03.1971 - 09.1976
N1103	60.5911	10.1956	NORSAR Array	NORSAR	03.1971 - 09.1976
N1201	60.8008	10.0386	NORSAR Array	NORSAR	03.1971 - 09.1976
N1303	61.0281	9.9381	NORSAR Array	NORSAR	03.1971 - 09.1976
N1403	61.1527	10.3090	NORSAR Array	NORSAR	03.1971 - 09.1976
NAO01	60.8442	10.8865	NORSAR Array	NORSAR/IMS	03.1971 -
NB201	61.0495	11.2939	NORSAR Array	NORSAR/IMS	03.1971 -
NB302	60.9158	11.3309	NORSAR Array	NORSAR	03.1971 - 09.1976
NB400	60.6738	11.1881	NORSAR Array	NORSAR	03.1971 - 09.1976
NB504	60.5961	10.7794	NORSAR Array	NORSAR	03.1971 - 09.1976
NB603	60.6986	10.4358	NORSAR Array	NORSAR	03.1971 - 09.1976
NB701	60.9415	10.5296	NORSAR Array	NORSAR	03.1971 - 09.1976
NBO00	61.0307	10.7774	NORSAR Array	NORSAR/IMS	03.1971 -
NC204	61.2759	10.7629	NORSAR Array	NORSAR/IMS	03.1971 -
NC303	61.2251	11.3690	NORSAR Array	NORSAR/IMS	03.1971 -
NC405	61.1128	11.7153	NORSAR Array	NORSAR/IMS	03.1971 -
NC503	60.9075	11.7981	NORSAR Array	NORSAR	03.1971 - 09.1976
NC602	60.7353	11.5414	NORSAR Array	NORSAR/IMS	03.1971 -
NC701	60.4939	11.5137	NORSAR Array	NORSAR	03.1971 - 09.1976
NC800	60.4756	11.0868	NORSAR Array	NORSAR	03.1971 - 09.1976
NC902	60.4084	10.6872	NORSAR Array	NORSAR	03.1971 - 09.1976
NCO00	61.3374	10.5854	NORSAR Array	NORSAR	03.1971 - 09.1976
NOR	81.6000	-16.6833	Nord	GEUS/GEOFON	08.2002
NRE0	60.7352	11.5414	NORES Array	NORSAR	10.1984 - 06.2002
NRIL	69.5049	88.4414	Norilsk	IRIS/IDA/IMS	12.1992 -
NSS	64.5307	11.9673	Namsos	NNSN	10.2001 -
OBN	55.1138	36.5687	Obninsk	IRIS/IDA	09.1988 -
PUL	59.7670	30.3170	Pulkovo	GEOFON	05.‘995 -
RGN	54.5477	13.3214	Rügen	GRSN/GEOFON	12.1995 -
RUE	52.4759	13.7800	Rüdersdorf	GRSN/GEOFON	01.2000 -
RUND	60.4135	5.3672	Rundemannen	NNSN	03.1997 - 03.2003
SCO	70.4830	-21.9500	Ittoqqortoormiit (Scoresbysund)	GEUS	05.1999 -
SFJ	66.9967	-50.6156	Sondre Stromfjord	GEUS/IRIS/USGS/GEOFON	03.1996 -
SPB4	78.1789	16.3482	Spitsbergen Array	NORSAR/IMS	11.1992 -
STU	48.7719	9.1950	Stuttgart	GEOFON/GRSN	04.1994 -
SUMG	72.5763	-38.4540	Summit Camp	GEOFON	06.2002 -
SUW	54.0125	23.1808	Suwalki	GEOFON	11.1995 -
TIXI	71.6490	128.8665	Tiksi	IRIS/USGS/IMS	08.1995 -
TRO	69.6345	18.9077	Tromsø	NNSN	03.2003 -
TRTE	58.3786	26.7205	Tartu	GEOFON	06.1996 - 04.2003
VSU	58.4620	26.7347	Vasula	GEOFON	04.2003 -
WLF	49.6646	6.1526	Walferdange	GEOFON	03. 1994 -
YAK	62.0308	129.6812	Yakutsk	IRIS/USGS/IMS	09.1993 -

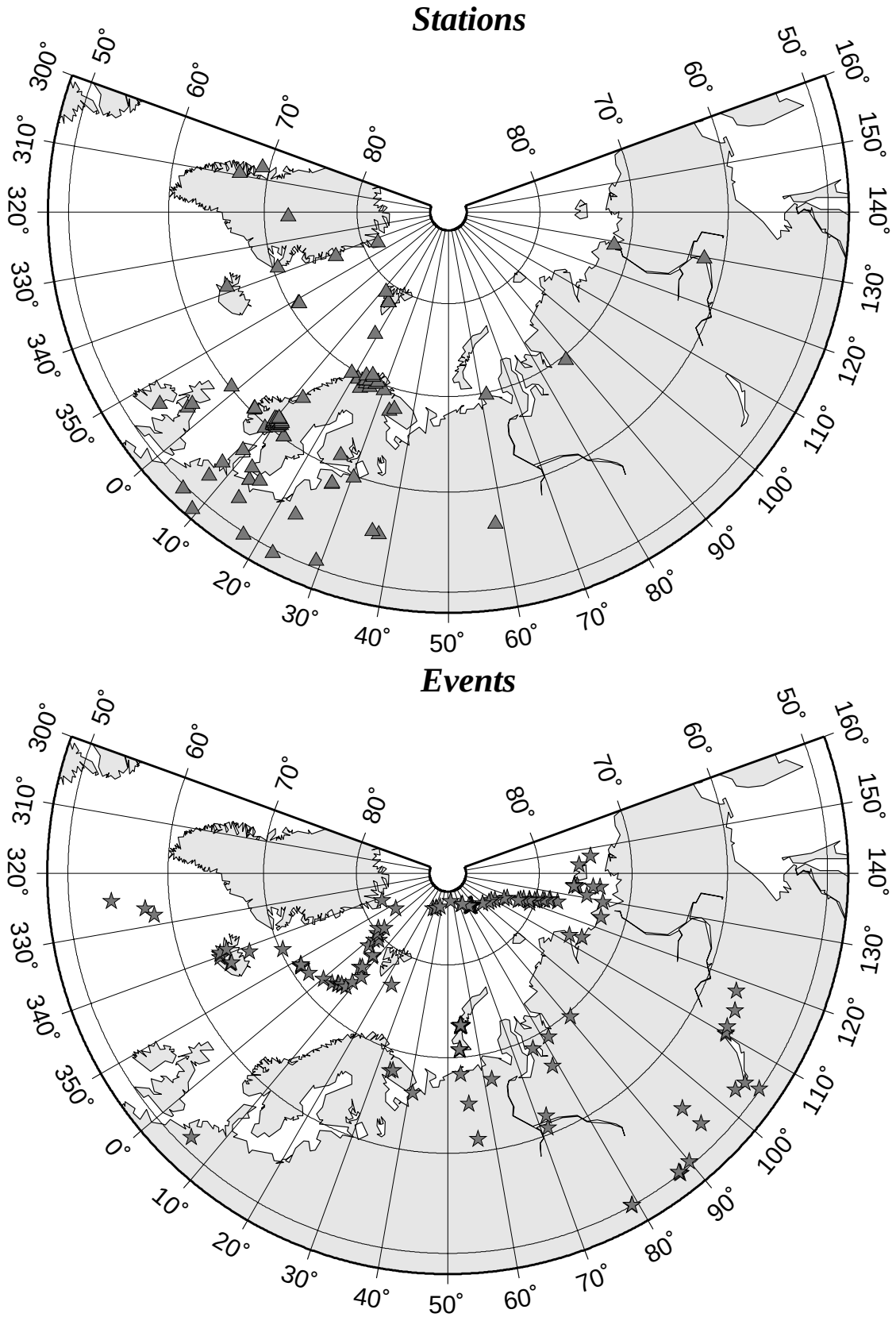

Fig. 6.3.1. The top map shows the seismic stations listed at Table 6.3.1 and the bottom map shows the distribution of the newly investigated seismic events as listed at Table 6.3.2.

Table 6.3.2. List with source parameters of the seismic events newly investigated during this study for measuring the group velocities of surface waves (Love and Rayleigh waves). A map with the event locations is shown in Fig. 6.3.1. All nuclear explosions investigated are marked with "expl".

Lat	Lon	Depth	Year	Month	Day	Time	mb	Ms	comment
61.2870	56.4660	0.0	1971	3	23	06:59:56.000	5.6	-	expl
73.3870	55.1000	0.0	1971	9	27	05:59:55.200	6.4	5.2	expl
73.3360	55.0850	0.0	1972	8	28	05:59:56.500	6.3	4.7	expl
52.3240	95.3660	33.0	1972	8	31	14:03:16.300	5.5	4.9	
73.3020	55.1610	0.0	1973	9	12	06:59:54.300	6.8	5.0	expl
70.7560	53.8720	0.0	1973	9	27	06:59:58.000	6.0	4.9	expl
64.7710	-21.0450	13.0	1974	6	12	17:55:08.700	5.5	5.3	
68.9130	75.8990	0.0	1974	8	14	14:59:58.300	5.5	-	expl
73.3660	55.0940	0.0	1974	8	29	09:59:55.500	6.4	5.0	expl
67.2330	62.1190	0.0	1974	8	29	14:59:59.600	5.2	-	expl
70.8170	54.0630	0.0	1974	11	2	04:59:56.700	6.7	5.3	expl
73.3690	54.6410	0.0	1975	8	23	08:59:57.900	6.4	4.9	expl
70.8430	53.6900	0.0	1975	10	18	08:59:56.300	6.7	5.1	expl
73.3510	55.0780	0.0	1975	10	21	11:59:57.300	6.5	-	expl
73.4040	54.8170	0.0	1976	9	29	02:59:57.400	5.8	4.5	expl
69.5320	90.5830	0.0	1977	7	26	16:59:57.600	4.9	-	expl
73.3760	54.5810	0.0	1977	9	1	02:59:57.500	5.7	-	expl
73.3360	54.7920	0.0	1978	8	10	07:59:57.700	5.9	4.3	
73.3800	54.6690	0.0	1978	9	27	02:04:58.200	5.6	4.5	expl
50.0460	78.9830	0.0	1978	11	4	05:05:57.500	5.6	4.2	expl
50.0530	79.0650	0.0	1979	7	7	03:46:57.400	5.8	-	expl
73.3690	54.7080	0.0	1979	9	24	03:29:58.300	5.7	-	expl
60.6770	71.5010	0.0	1979	10	4	15:59:57.900	5.4	-	
73.3380	54.8070	0.0	1979	10	18	07:09:58.300	5.8	-	expl
71.1920	-8.0300	10.0	1979	11	20	17:36:01.200	5.6	5.4	
73.3530	54.9970	0.0	1980	10	11	07:09:57.000	5.8	3.8	expl
68.2050	53.6560	0.0	1981	5	25	04:59:57.300	5.5	-	
73.3170	54.8120	0.0	1981	10	1	12:14:56.800	5.9	3.8	expl
69.2060	81.6470	0.0	1982	9	4	17:59:58.400	5.2	3.5	
73.3920	54.5590	0.0	1982	10	11	07:14:58.200	5.6	3.6	expl
73.3830	54.9130	0.0	1983	8	18	16:09:58.600	5.9	4.2	expl
73.3480	54.4950	0.0	1983	9	25	13:09:57.700	5.8	-	expl
65.0250	55.1870	0.0	1984	8	11	18:59:57.800	5.3	-	
61.8760	72.0920	0.0	1984	8	25	18:59:58.600	5.4	-	
67.7740	33.6880	0.0	1984	8	27	05:59:57.000	4.5	-	expl
73.3700	54.9550	0.0	1984	10	25	06:29:57.700	5.9	4.7	expl
65.9700	40.8630	0.0	1985	7	18	21:14:57.400	5.0	-	expl
63.8500	-19.7280	8.0	1987	5	25	11:31:54.300	5.8	5.8	
82.2290	-17.5560	10.0	1987	7	11	06:15:51.000	5.5	5.0	
73.3390	54.6260	0.0	1987	8	2	01:59:59.800	5.8	3.4	expl
74.6550	130.9620	10.0	1988	1	1	14:36:09.500	5.1	4.6	
77.6010	125.4510	10.0	1988	3	21	23:31:21.600	6.0	6.0	
73.3640	54.4450	0.0	1988	5	7	22:49:58.100	5.6	3.8	expl
66.3160	78.5480	0.0	1988	8	22	16:19:58.200	5.3	-	expl
73.3870	54.9980	0.0	1988	12	4	05:19:53.000	5.9	4.6	expl
71.1340	-7.6340	10.0	1988	12	13	04:01:38.900	5.7	5.6	
50.1030	105.3600	36.0	1989	5	13	03:35:02.800	5.6	5.6	
71.4320	-4.3710	10.0	1989	6	9	12:19:35.700	5.6	5.4	
76.1180	134.5780	10.0	1989	8	5	06:55:50.900	5.3	5.0	
76.1660	134.3460	13.0	1989	8	5	10:49:23.300	4.6	-	
76.1750	134.2460	10.0	1989	9	26	00:18:50.000	4.5	-	
80.6380	121.7610	31.0	1989	10	3	23:09:53.800	5.2	4.9	
80.5880	122.1320	10.0	1989	11	17	04:05:18.500	5.1	5.3	
73.3250	134.9090	18.0	1990	3	13	00:32:59.100	5.5	4.9	
74.2250	8.8280	29.0	1990	5	27	21:49:35.400	5.5	5.7	
75.0920	113.0960	33.0	1990	6	9	18:24:34.200	5.0	5.1	
64.6550	-17.6170	10.0	1990	9	15	23:07:42.800	5.5	5.2	
73.3610	54.7070	0.0	1990	10	24	14:57:58.100	5.7	4.0	expl
79.8490	123.8840	10.0	1991	3	22	17:02:19.500	4.7	4.1	
84.4010	108.2490	27.0	1991	6	11	07:16:34.400	5.5	5.3	

Lat	Lon	Depth	Year	Month	Day	Time	mb	Ms	comment
51.1530	5.7980	21.0	1992	4	13	01:20:00.800	5.5	5.2	
81.2460	121.2700	32.0	1992	6	8	09:30:16.100	5.1	4.6	
64.7800	-17.5940	10.0	1992	9	26	05:45:50.600	5.5	5.4	
86.9410	56.0730	10.0	1993	2	23	11:56:27.100	4.7	4.6	
64.5780	-17.4820	9.0	1994	5	5	05:14:49.700	5.7	5.2	
56.7610	117.9000	12.0	1994	8	21	15:55:59.200	5.8	5.8	
78.3020	2.3020	10.0	1995	3	9	07:04:22.100	5.1	4.4	
50.3720	89.9490	14.0	1995	6	22	01:01:19.000	5.5	5.2	
51.9610	103.0990	12.0	1995	6	29	23:02:28.200	5.6	5.5	
75.9840	6.9560	10.0	1995	10	4	09:17:30.200	5.1	4.9	
56.1000	114.4950	22.0	1995	11	13	08:43:14.500	5.9	5.6	
72.6440	3.4880	10.0	1995	12	8	07:41:12.700	5.2	5.2	
75.8200	134.6190	10.0	1996	6	22	16:47:12.910	5.6	5.5	
77.8600	7.5640	10.0	1996	8	20	00:11:00.340	5.3	5.0	
77.7460	7.8770	10.0	1997	2	6	14:41:51.750	5.3	-	
78.5100	125.5150	10.0	1997	4	16	08:42:27.550	4.8	4.3	
78.4450	125.8210	10.0	1997	4	19	15:26:33.480	5.7	5.0	
73.4170	7.9880	10.0	1997	10	6	21:13:10.380	5.0	-	
79.8880	1.8560	10.0	1998	3	21	16:33:11.000	5.9	6.1	
72.8260	129.5830	10.0	1998	8	23	09:59:02.970	4.5	-	
86.2830	75.6090	10.0	1998	10	18	22:09:19.160	5.2	4.6	
85.6410	86.1000	10.0	1999	2	1	04:52:40.810	5.1	4.7	
85.7340	84.4390	10.0	1999	2	1	09:56:35.020	5.1	5.2	
85.6050	85.8370	10.0	1999	2	1	11:55:15.070	4.5	-	
85.5710	87.1410	10.0	1999	2	1	11:56:00.800	5.1	5.5	
85.5730	87.0370	10.0	1999	2	19	19:10:00.540	5.1	5.0	
86.2780	73.3940	10.0	1999	2	22	08:02:11.170	5.2	4.8	
51.6040	104.8640	10.0	1999	2	25	18:58:29.400	5.9	5.5	
85.6860	86.0340	10.0	1999	3	1	17:46:46.340	5.0	5.0	
85.6920	84.7970	10.0	1999	3	13	01:26:33.540	5.3	5.1	
85.6340	86.8190	10.0	1999	3	21	15:24:07.840	5.4	5.1	
55.8960	110.2140	10.0	1999	3	21	16:16:02.200	5.5	5.7	
85.6820	85.7360	10.0	1999	3	28	21:32:29.650	4.4	-	
85.6440	86.2590	10.0	1999	3	28	21:33:44.090	5.0	5.1	
85.6480	86.5310	10.0	1999	4	1	10:47:53.010	5.1	5.1	
73.2150	6.6500	10.0	1999	4	13	02:09:22.270	5.0	4.7	
85.6720	84.8300	10.0	1999	4	26	13:20:07.620	5.2	4.9	
85.6320	86.1460	10.0	1999	5	18	20:20:16.060	5.1	5.3	
85.6050	86.5260	10.0	1999	5	26	23:56:32.670	5.1	4.6	
73.0170	5.1870	10.0	1999	6	7	16:10:33.630	5.3	5.4	
73.0770	5.4530	10.0	1999	6	7	16:35:46.700	5.2	5.3	
85.6040	83.7040	10.0	1999	6	11	23:54:52.000	5.1	4.5	
85.6770	85.7720	10.0	1999	6	18	19:47:25.180	5.3	4.8	
70.2800	-15.3510	10.0	1999	7	1	02:08:02.010	4.9	-	
85.7410	83.2640	10.0	1999	7	8	19:25:10.520	5.0	4.6	
72.2610	0.3960	10.0	1999	8	3	13:55:41.410	5.0	5.1	
67.8630	34.3790	10.0	1999	8	17	04:44:35.950	4.6	-	
79.2210	124.3970	10.0	1999	10	27	05:05:07.180	4.8	4.5	
55.8300	110.0290	10.0	1999	12	21	11:00:48.870	5.5	5.0	
80.6150	122.1300	10.0	1999	12	26	08:39:48.390	4.7	-	
80.5820	122.2510	10.0	1999	12	30	06:46:55.250	4.7	4.4	
79.8020	123.0760	10.0	2000	1	16	12:29:12.630	4.5	3.8	
75.2710	10.1950	10.0	2000	2	3	15:53:12.960	5.5	5.0	
79.8900	0.4380	10.0	2000	2	12	09:05:06.630	5.0	4.7	
71.1900	-8.2630	10.0	2000	5	21	19:58:47.410	5.3	5.6	
63.9660	-20.4870	10.0	2000	6	17	15:40:41.730	5.7	6.6	
63.9800	-20.7580	10.0	2000	6	21	00:51:46.880	6.1	6.6	
74.3330	146.9720	10.0	2000	7	10	04:17:36.830	4.6	3.9	
78.9680	124.4680	10.0	2000	9	16	17:45:17.820	4.6	-	
54.7070	94.9830	33.0	2000	10	27	08:08:53.540	5.6	5.3	
81.5320	120.2790	27.3	2000	12	31	01:45:03.240	5.1	4.5	
80.0380	122.7240	10.0	2001	4	8	02:59:03.880	4.5	-	
80.4640	120.0940	10.0	2001	5	1	23:44:57.170	4.5	-	
82.9330	117.5090	10.0	2001	5	30	15:19:04.350	4.7	-	
72.6750	124.0160	61.5	2001	6	8	04:59:05.250	4.7	-	

Lat	Lon	Depth	Year	Month	Day	Time	mb	Ms	comment
79.5140	4.1880	10.0	2001	7	16	14:09:29.240	5.0	4.5	
80.8480	0.7680	10.0	2001	12	8	06:44:22.020	5.1	4.8	
85.8580	27.6810	10.0	2002	5	3	11:19:20.320	4.1	-	
86.0050	31.5950	10.0	2002	5	3	11:20:51.540	5.2	5.4	
85.9720	31.1490	10.0	2002	5	3	15:33:34.880	5.1	5.1	
86.2760	37.1770	10.0	2002	5	28	15:39:01.550	4.9	4.7	
75.6340	143.7460	10.0	2002	6	4	00:05:07.170	4.8	-	
84.0830	110.6900	10.0	2002	6	9	21:20:38.750	4.5	-	
83.1360	-6.0780	10.0	2002	9	11	04:50:32.860	5.2	5.2	
66.9380	-18.4560	10.0	2002	9	16	18:48:26.720	5.5	5.7	
58.3110	-31.9460	10.0	2002	10	7	20:03:54.580	4.9	5.5	
57.4490	-33.3440	10.0	2003	2	1	18:47:52.150	5.3	5.5	
71.1220	-7.5770	10.0	2003	6	19	12:59:24.410	5.6	5.0	
76.3720	23.2820	10.0	2003	7	4	07:16:44.720	5.7	5.1	
73.2730	6.4210	10.0	2003	8	30	01:04:42.340	5.0	4.8	
56.0620	111.2550	10.0	2003	9	16	11:24:52.220	5.2	5.7	
80.3140	-1.8280	10.0	2003	9	22	20:45:16.910	5.2	4.7	
50.0380	87.8130	16.0	2003	9	27	11:33:25.080	6.5	7.5	
50.0910	87.7650	10.0	2003	9	27	18:52:46.980	6.1	6.6	
50.2110	87.7210	10.0	2003	10	1	01:03:25.240	6.3	7.1	
79.1410	2.3290	10.0	2003	10	7	02:36:54.440	5.1	4.6	
74.0800	134.8210	10.0	2003	12	7	09:16:12.640	5.0	4.4	
84.4750	105.2150	10.0	2004	1	19	07:22:52.910	5.5	5.2	
71.0670	-7.7470	12.2	2004	4	14	23:07:39.940	5.8	5.6	
81.7290	119.2920	10.0	2004	6	24	22:12:37.160	4.7	-	
54.1310	-35.2590	10.0	2004	7	1	09:20:44.140	5.4	5.5	
73.8300	114.4820	10.0	2004	10	2	11:06:01.470	4.5	-	
83.2630	115.9400	10.0	2004	11	13	21:28:01.450	4.6	-	
76.1690	7.5280	10.0	2004	11	27	06:38:29.290	5.0	4.5	
84.9480	99.3100	10.0	2005	3	6	05:21:43.430	6.1	6.2	

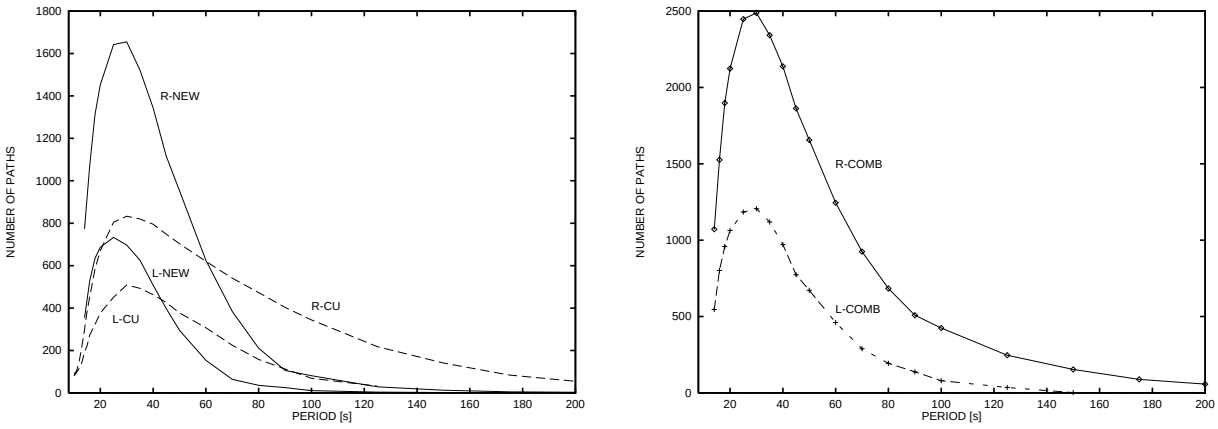

Fig. 6.3.2. The figure on the left shows the number of observed ray paths, on which Love- (L) and Rayleigh-wave (R) group velocities were measured for the preselected Colorado University data set (dashed lines, R-CU and L-CU) and during this new study (R-NEW and L-NEW). The figure on the right shows the number of ray paths in the joint data set used for the inversions in this study.

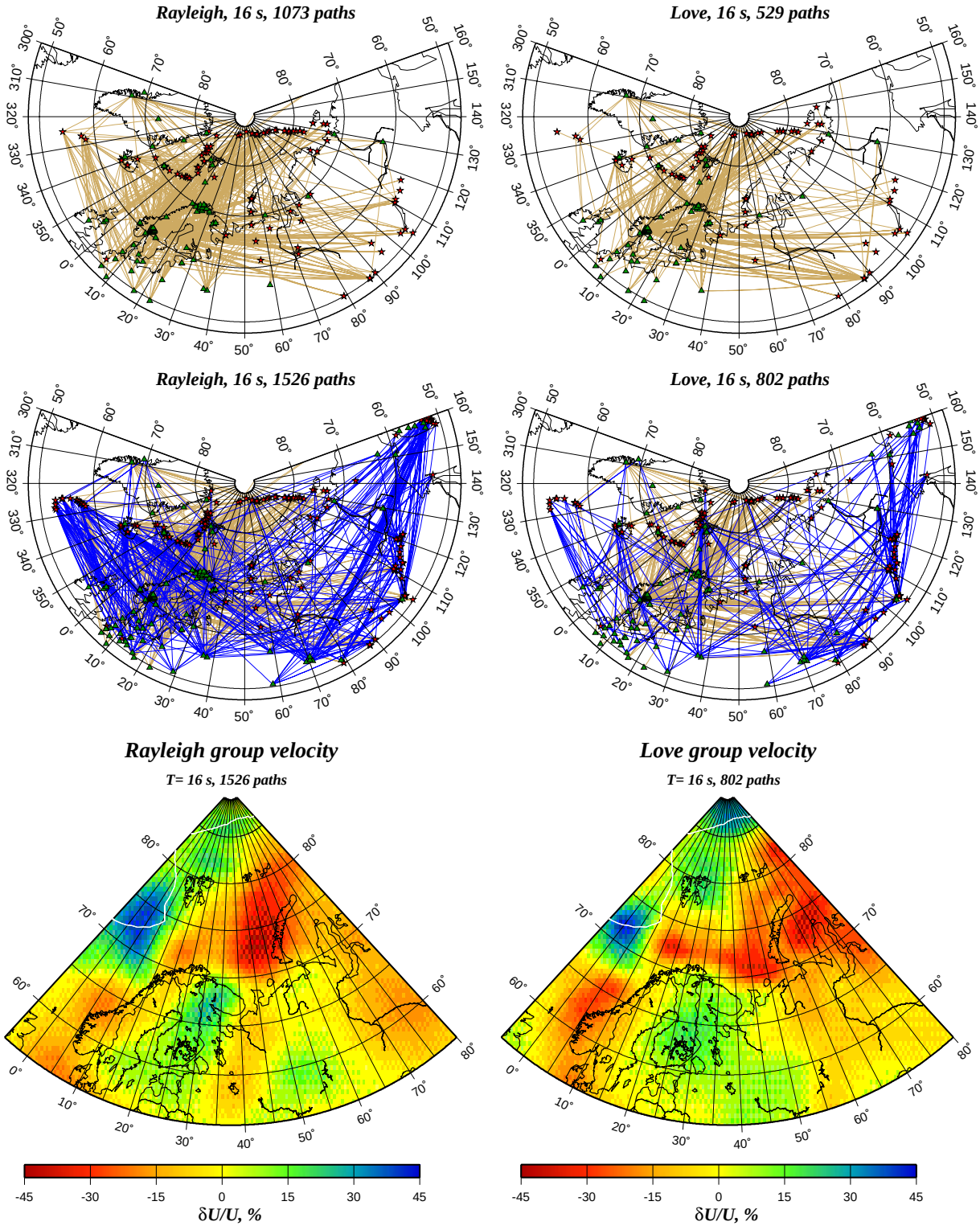

Fig. 6.3.3. Results of the 2D inversion for the group velocities of Love (on the right) and Rayleigh waves (on the left) with a period of 16 s. The two maps at the top show the ray coverage of the newly analyzed data. The two maps in the middle show the same rays plus the rays for the data from the preselected CU data set (blue). The two maps at the bottom present the 2D distribution of the inverted group velocities as deviations from the average velocity (in percent).

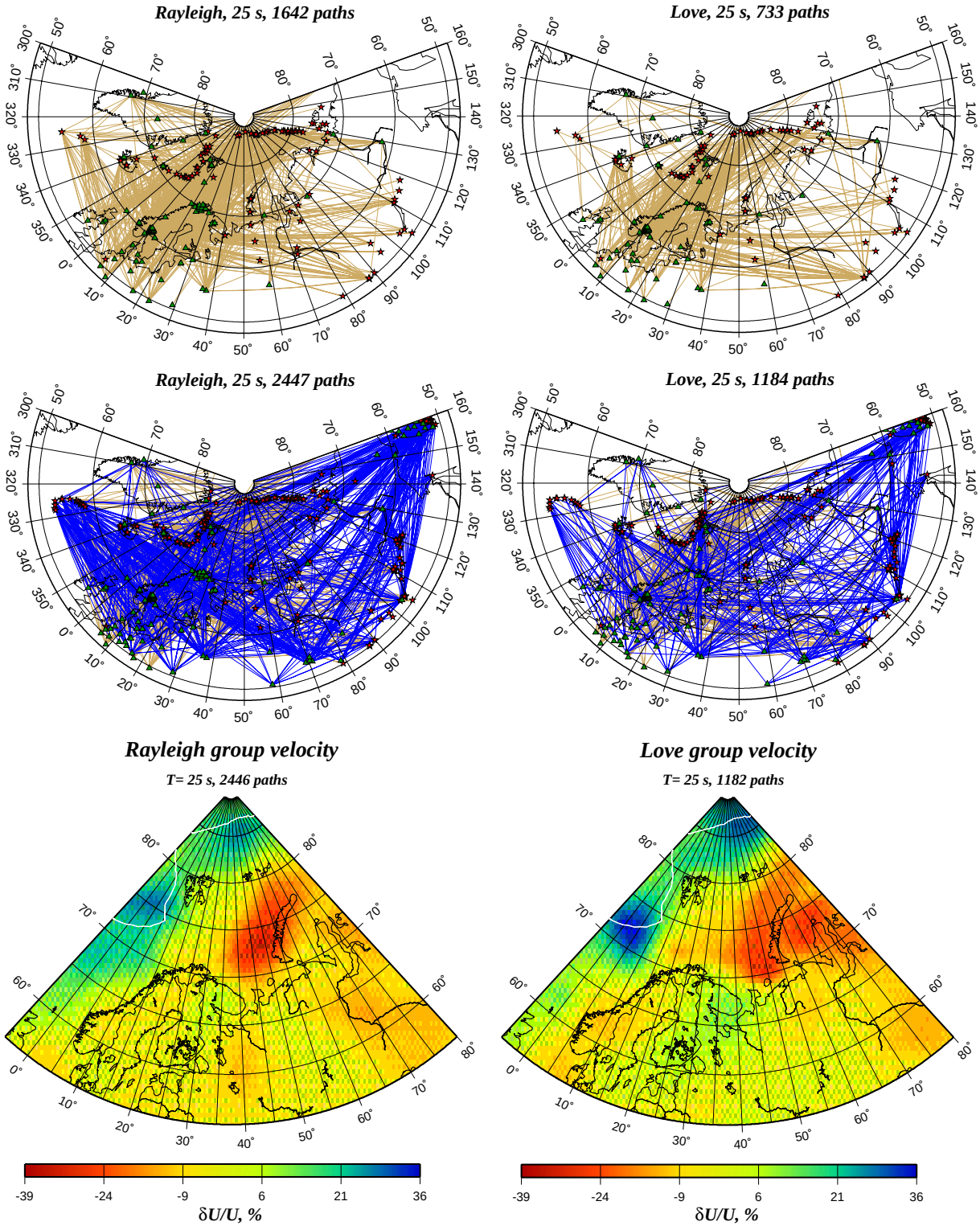

Fig. 6.3.4. Results of the 2D inversion for the group velocities of Love (on the right) and Rayleigh waves (on the left) with a period of 25 s. The two maps at the top show the ray coverage of the newly analyzed data. The two maps in the middle show the same rays plus the rays for the data from the preselected CU data set (blue). The two maps at the bottom present the 2D distribution of the inverted group velocities as deviations from the average velocity (in percent).

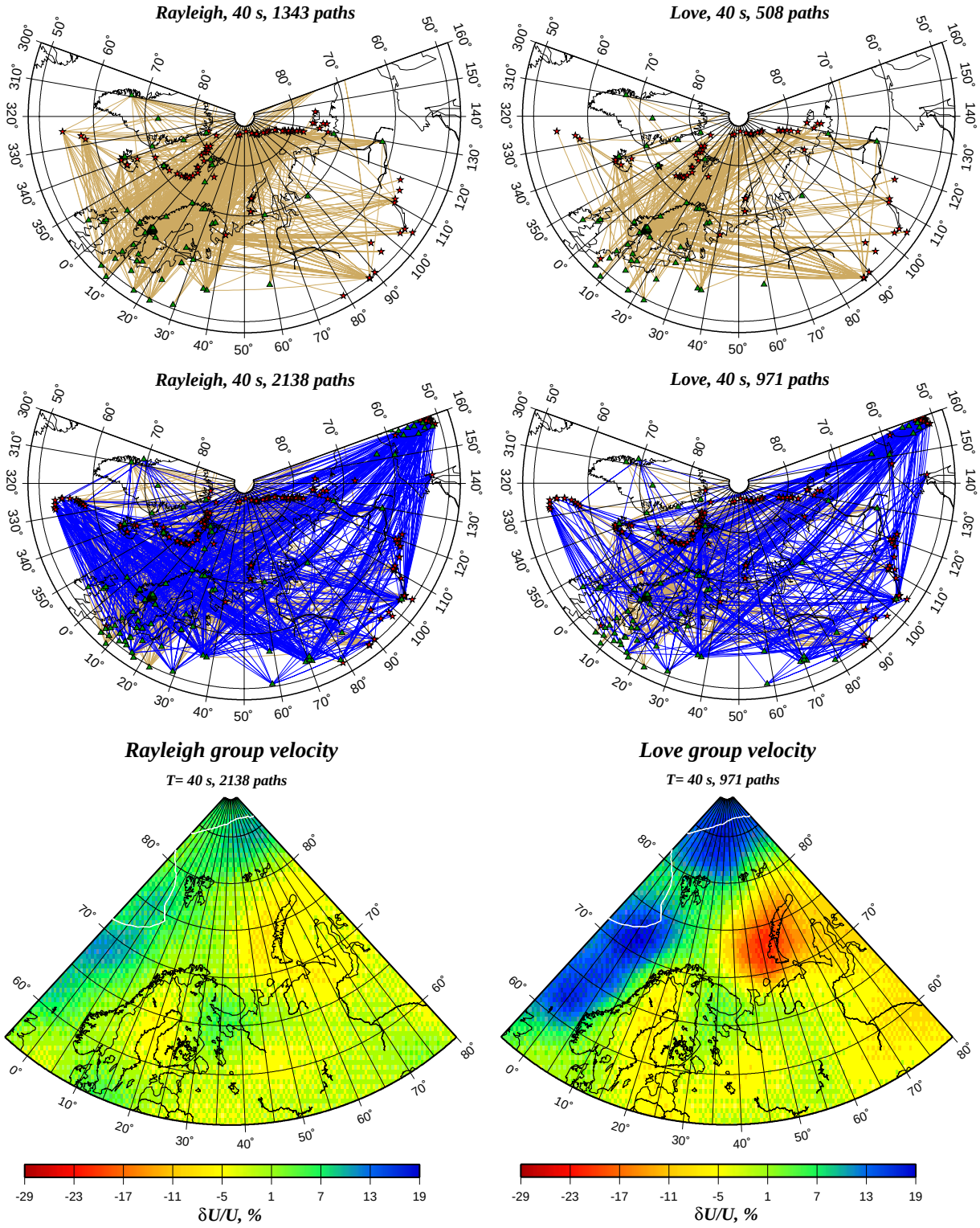

Fig. 6.3.5. Results of the 2D inversion for the group velocities of Love (on the right) and Rayleigh waves (on the left) with a period of 40 s. The two maps at the top show the ray coverage of the newly analyzed data. The two maps in the middle show the same rays plus the rays for the data from the preselected CU data set (blue). The two maps at the bottom present the 2D distribution of the inverted group velocities as deviations from the average velocity (in percent).

6.4 Combined seismic/infrasonic processing: A case study of explosions in NW Russia

6.4.1 Introduction

This paper contains results from a continued study of combining seismic and infrasonic recordings for detection and characterization of seismic events at local and regional distances. We present results from an analysis of several recent surface explosions in the Kola peninsula near the Norwegian border. At least two of the explosions were reported felt/heard over a large area in the Varanger peninsula, northern Norway, at an epicentral distance of more than 100 km. The explosions were presumably carried out for the purpose of destroying old ammunition, and generated unusually strong infrasonic signals in addition to seismic signals. Not unexpectedly, the infrasonic signals were well recorded on the infrasound array in Apatity, but more interestingly, they were also clearly recorded on the seismic sensors at the ARCES and Apatity arrays (both at about 250 km distance from the source area). We used the recordings to make a location estimate based upon the infrasonic detections (on the seismic sensors) at these two arrays, and found that the locations matched closely the locations obtained through standard seismic data analysis. This indicates an interesting potential for joint two-array infrasonic processing, and this concept will be further developed once the IMS infrasound array near ARCES has been established (expected in 2006).

6.4.2 Data sources

The Apatity seismic array was originally installed in 1992 as a cooperative project between the Kola Regional Seismological Centre (KRSC) and NORSAR. It comprises 9 elements deployed in two concentric rings together with a center element, and has a diameter of 1 km. In 1996, KRSC became engaged in infrasonic research and development. As part of this effort, a small-aperture microbarographic array was installed in conjunction with the seismic array, with data digitized at the array site and transmitted in real time to a processing center in Apatity. A total of three infrasound sensors are installed in the innermost ring of the array, forming a triangle of approximately 500 m diameter. The sensors are differential microbarographs of model K-304-AM. The frequency working range is 0.01-10 Hz, and the sensitivity is 37.5 mV/Pa. The geometry of the combined seismic/infrasound array is shown in Fig. 6.4.1. A brief description of the Apatity infrasound system and initial results from the infrasound array operation has been presented by Vinogradov and Ringdal (2003).

The ARCES seismic array (IMS station PS28) is located in northern Norway (see Fig. 6.4.2), and will be supplemented by an infrasonic array (IS37) in the near future. Joint processing of seismic data from ARCES and Apatity has been carried out for a number of years, and has resulted in improved understanding of many topics related to two-array detection, location and characterization of small seismic events recorded at regional distances. The explosions analyzed in this paper provide the first opportunity to carry out joint two-array processing of infrasonic data, since these explosions generated unusually strong sound waves, and these sound waves were clearly recorded at the seismic sensors of the ARCES array.

The explosions forming the database for this study are listed in Table 6.4.1, which contains both the event locations from the NORSAR reviewed regional seismic bulletin and locations estimated from joint two-array infrasonic processing as described later in this paper.

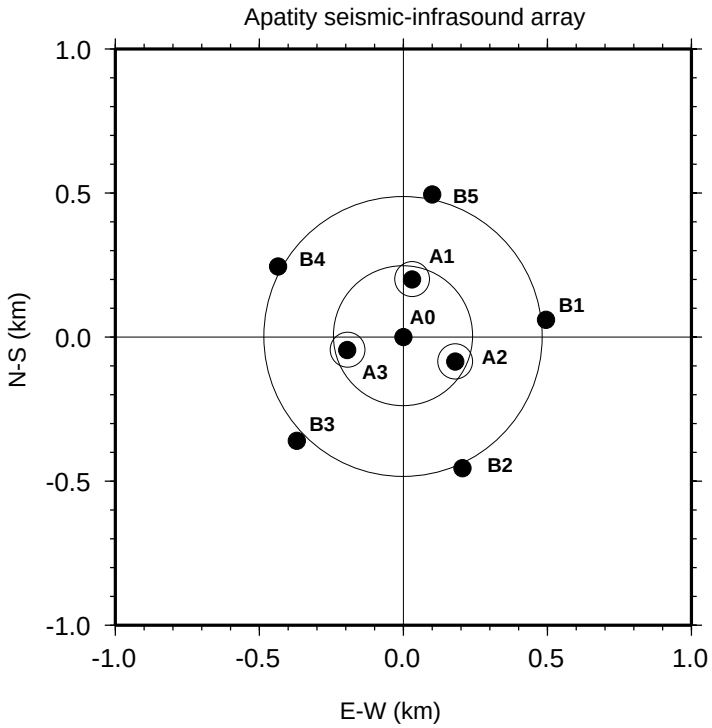

Fig. 6.4.1. *Configuration of the Apatity seismic-infrasound array. Seismometers are shown as filled circles, with the location of the three infrasonic sensors (A1, A2 and A3) marked as small circles. The two concentric circles have diameters of 500 m and 1000 m respectively.*

Table 6.4.1. List of analyzed events.

	NORSAR reviewed bulletin					This paper	
No	**Date**	**Origin time**	**ML**	**Lat. N**	**Lon. E**	**Lat. N**	**Lon. E**
1	2005/03/10	19.03.38.9	1.44	69.47	31.65	69.71	32.11
2	2005/03/10	19.03.38.9	1.11	69.46	31.56	69.71	32.07
3	2005/03/15	16.17.24.8	1.78	69.42	31.56	69.60	31.79
4	2005/03/15	16.44.00.6	1.21	69.52	31.75	69.62	31.79
5	2005/03/17	14.48.24.2	1.65	69.55	31.86	69.60	31.73
6	2005/03/17	15.16.09.4	1.14	69.47	31.74	69.63	31.64

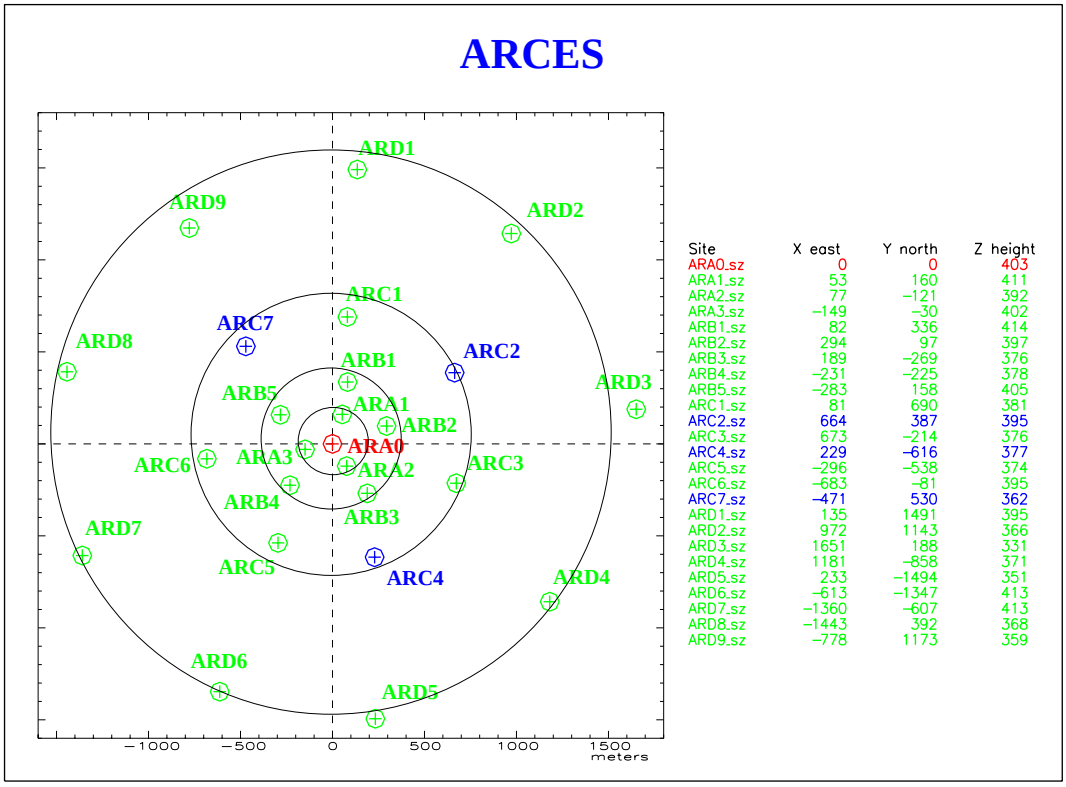

Fig. 6.4.2. *ARCES array configuration. The four circles correspond to the A, B, C and D-rings as discussed in the text.*

6.4.3 Data analysis

Detection processing

The regional processing system at the NORSAR Data Center (Ringdal and Kværna, 2004) is currently focused on seismic phases, and comprises STA/LTA detectors applied in parallel to a number of array beams in various filter bands. Although the beam set is not tuned to sound velocities, sound waves (if they are recorded with sufficient signal-to-noise ratio) will still be detected by the "incoherent" beams in the beam set.

In the present case, it turns out that the on-line detector for the ARCES array did in fact detect the sound waves from the six events. As an example, Fig. 6.4.3 shows selected individual ARCES channels for Event 5 in the data base, and we can see that the SNR of the sound waves is at least as good as for the seismic waves. Fig. 6.4.4 and 6.4.5 show the frequency-wavenumber solutions for the P-wave and the sound wave. The phase velocities are very different, 7.25 km/s for the P-wave, and 0.34 km/s for the sound wave. Thus, there is no problem in identifying the sound waves using apparent phase velocity as a criterion.

.

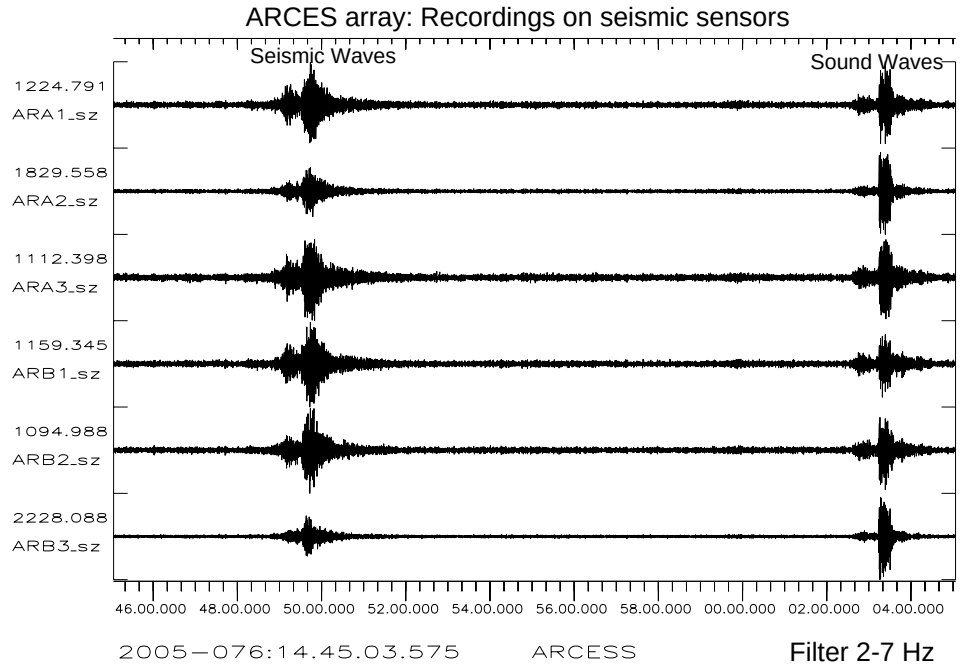

Fig. 6.4.3. *ARCES waveforms for one of the explosions discussed in the text (Event 5 in Table 6.4.1). Note the clear recording of both the seismic P and S waves and the sound waves, which appear about 14 minutes later.*

Table 6.4.2. Results from estimating the azimuth of the sound waves by f-k analysis.

Event no.	Configuration (diameter in parentheses)				
	ARCES 1 (3 km)	ARCES 2 (1.5 km)	ARCES 3 (0.7 km)	ARCES 4 (0.3 km)	Apatity (0.4 km)
1	82.91	82.45	81.92	81.59	351.67
2	83.24	82.55	82.40	82.31	351.31
3	86.58	85.34	84.76	84.27	348.14
4	85.78	84.75	84.29	83.64	348.31
5	85.79	85.47	84.69	84.25	347.48
6	85.69	84.58	83.52	82.70	346.90

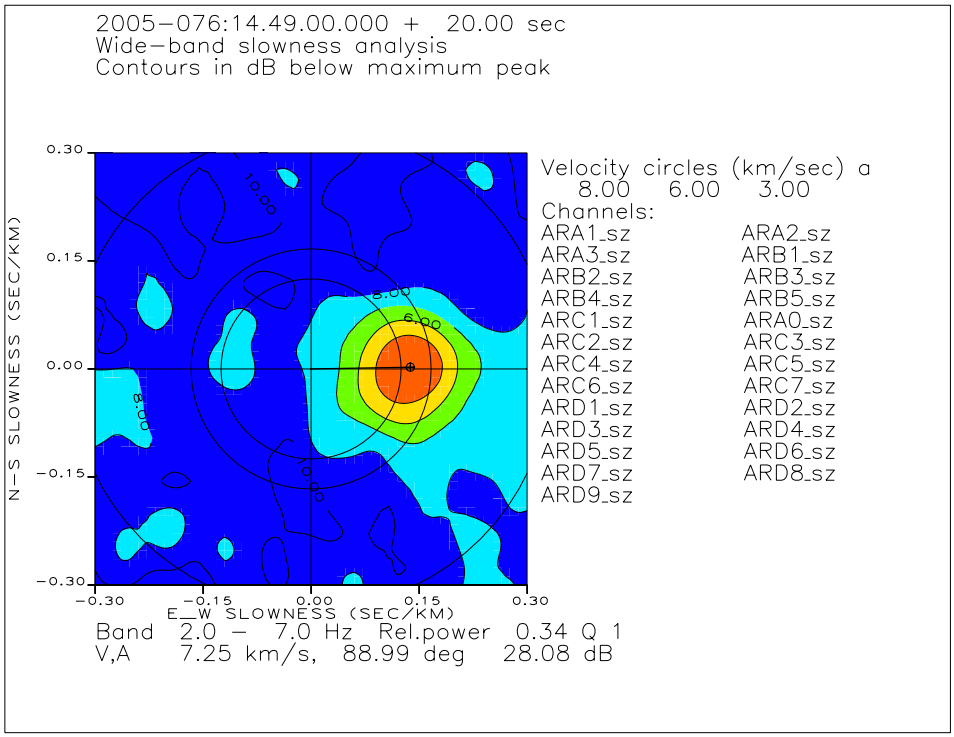

Fig. 6.4.4. *ARCES f-k plot of the P-phase for Event 5. Phase velocity is 7.25 km/s and the azimuth is 88.99 degrees.*

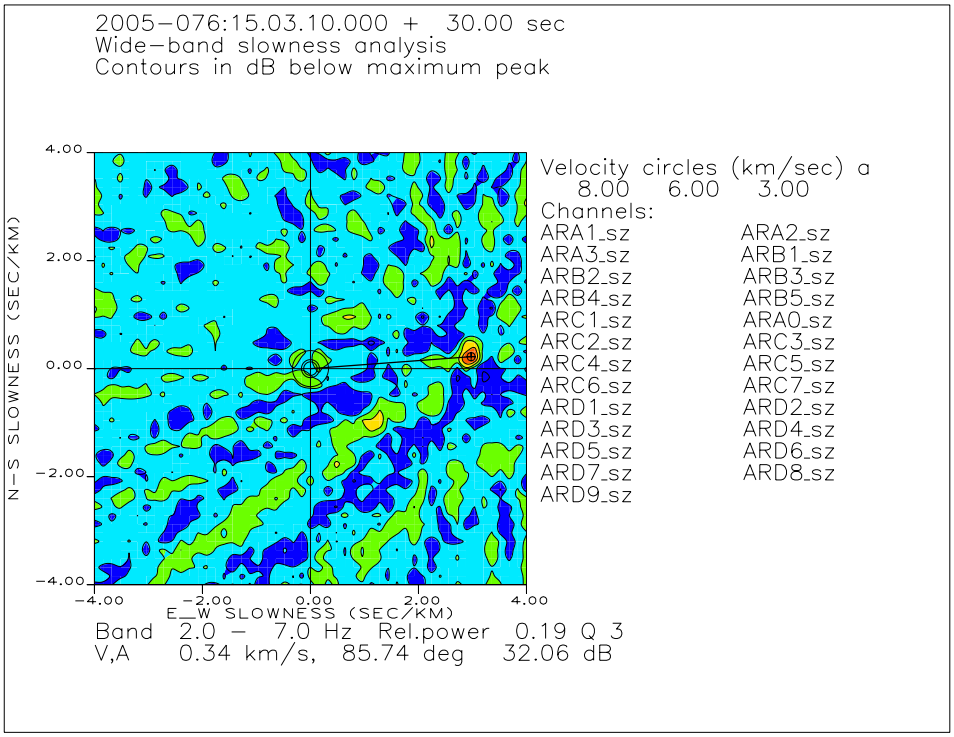

Fig. 6.4.5. *ARCES f-k plot of the sound phase for Event 5. The phase velocity is 0.34 km/s, which corresponds to sound velocity. The azimuth is 85.74 degrees.*

We also note that the azimuths of the P-phase and the sound phase are quite similar, and it would therefore be feasible to associate these phases automatically to the same event. This is currently not done in the NORSAR processing system, but is planned for implementation once the infrasonic array near ARCES is established. We will discuss the azimuth estimation of the infrasonic waves later in this paper.

Fig. 6.4.6 shows Apatity array recordings of the same event (Event 4). In this figure, we display three seismic sensors along with the three infrasonic sensors. As was the case for ARCES, the seismic sensors show both the seismic phases and the sound phase quite clearly. The infrasonic sensors show only the sound phase, and the SNR for this phase is (not unexpectedly) considerable higher than for the same phase on the seismic sensors.

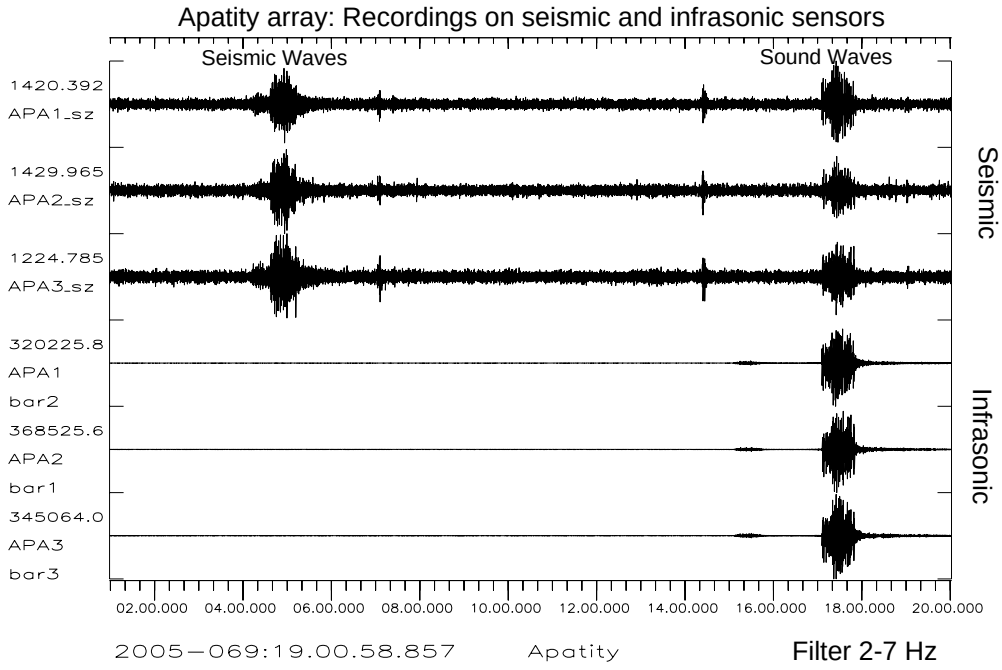

Fig. 6.4.6. *Recordings by three Apatity seismic sensors (top) and the three infrasonic sensors (bottom) for Event 5.*

Signal characteristics

When comparing the waveforms of the six events, we can make some interesting observations. In Fig. 6.4.7, we show the seismic phases for each event as recorded by the ARCES B3 sensor. These seismic recordings are quite similar, although the SNR shows some variation.

This observation can be contrasted with Figure 6.4.8 (for Apatity) and 6.4.9 (for ARCES), which show the infrasonic phase for the six events. For Apatity, we have selected infrasound channel Bar 2, and for ARCES the seismic channel B3. The channels are lined up according to the origin time of each event. There are several striking features: First, the apparent "arrival times" are quite different (by up to 20 seconds). This may not be very significant, since we do not know the exact locations of the explosions, and a time difference in sound wave travel time of 20 seconds corresponds to only 6-7 km in epicentral distance difference. In addition, sound

velocities in the atmosphere are quite variable due to changes in temperature, wind direction and air pressure. A second striking feature in the two figures is the considerable differences in signal shapes and duration. There were two explosions for each of the days 10 March, 15 March and 17 March. In each case, the first explosion is somewhat stronger, and has a long, drawn-out infrasonic signal with no clearly identifiable multiple phases. In contrast, the second explosion for each day shows two clearly distinct infrasonic phase arrivals on Apatity recordings, each with short duration. The ARCES recordings for these events are also of short duration, and show multiple phases for one of the events (Event 4).

Fig. 6.4.10 and 6.4.11 show the three infrasound sensors of the Apatity array for the two explosions of 17 March (Event 5 and Event 6). We note that the signals are extremely coherent across the array for each event. This is not surprising, and is a common feature for observed infrasound signals at this array. Furthermore, in view of the slow phase velocity, it is not surprising that the time delay of phase arrivals across the three sensors is large enough to be noticed. For this reason, f-k analysis can be expected to produce reliable velocity/azimuth estimates, even for a small array (less than 500 m in diameter).

It is interesting to note that the pairs of events for each day were separated in time by only approximately one half hour. Therefore, the atmospheric conditions would have been essentially the same for each pair. The seismic recordings displayed in Fig. 6.4.7 indicate no evidence of any significant difference in source function for the events, except that the first explosion of each pair is somewhat larger than the second explosion. We have at present no good explanation for the observed differences in the infrasonic waveforms.

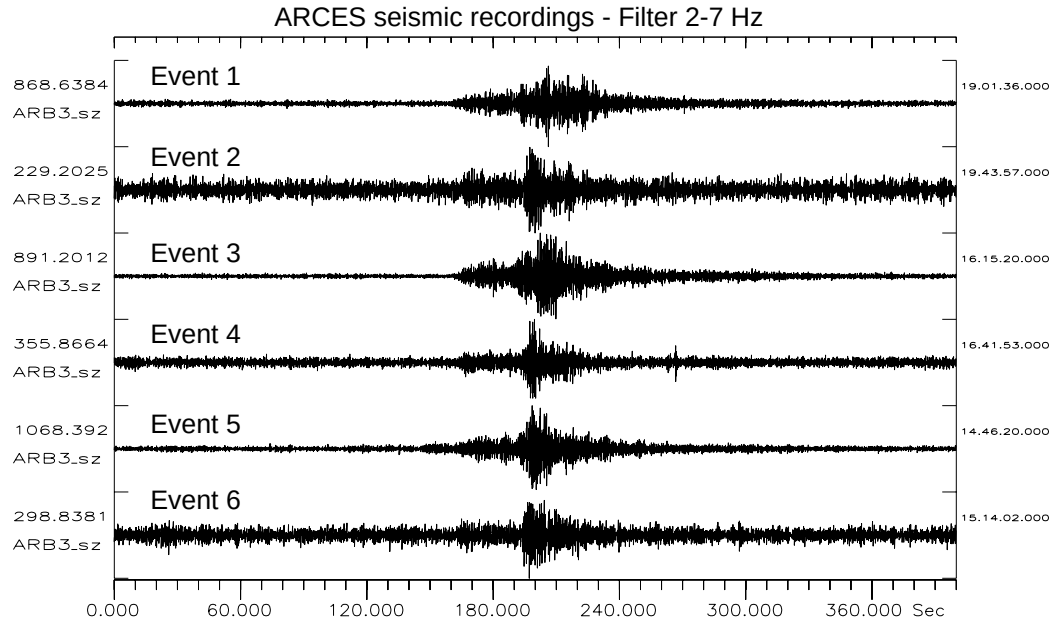

Fig. 6.4.7. *ARCES seismic recordings of the six events in the database.*

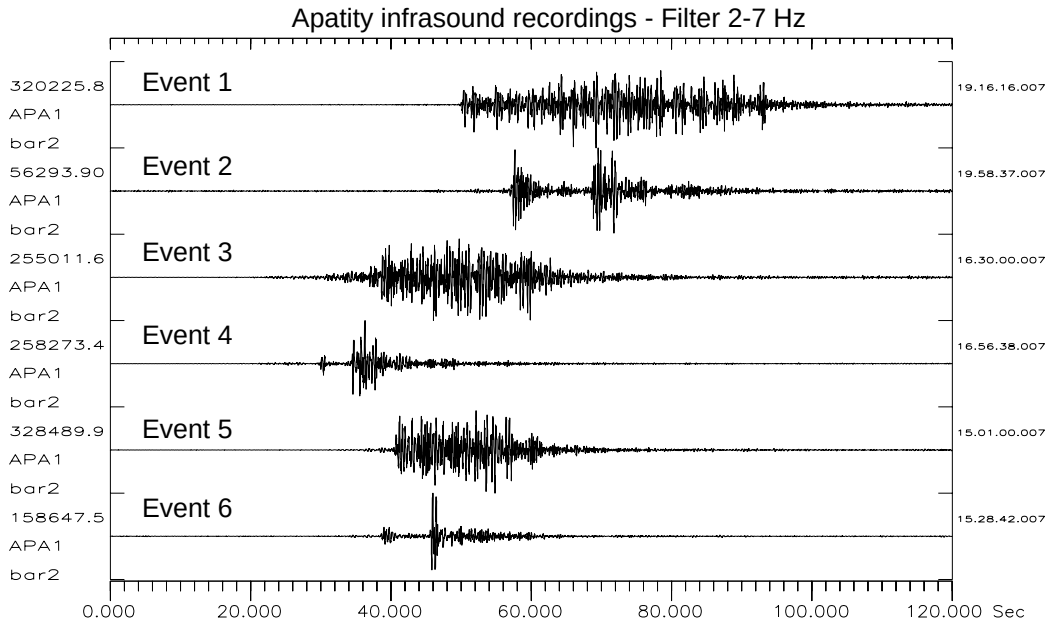

Fig. 6.4.8. *Apatity infrasound recordings of the six events in the database.*

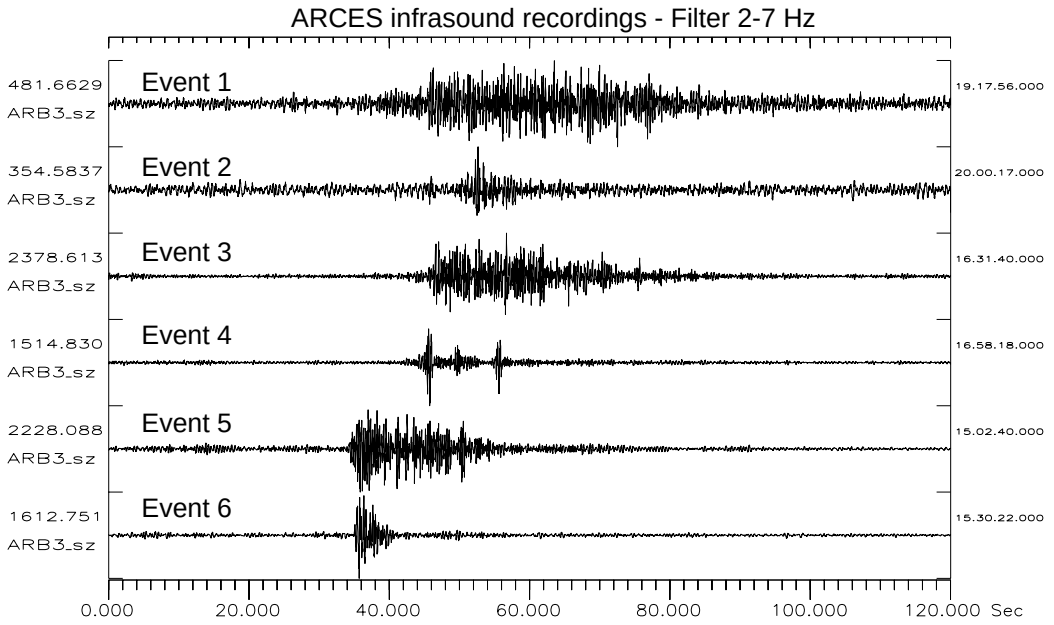

Fig. 6.4.9. *ARCES recordings on seismometer B3 of the infrasound phases for the six events in the database.*

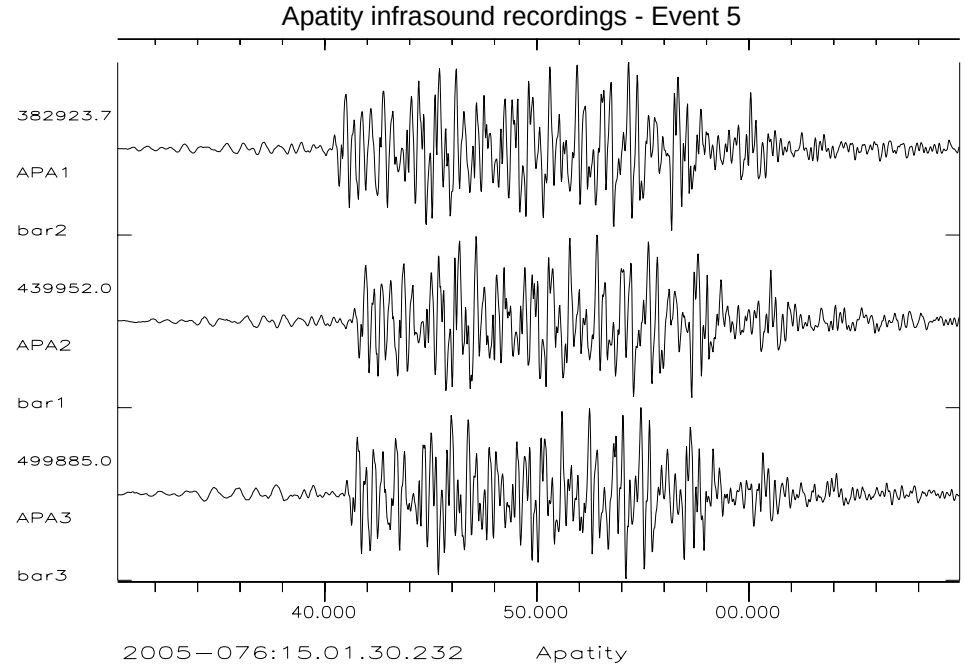

Fig. 6.4.10. *Apatity infrasound recordings of Event 5 in the database. The data are filtered in the frequency band 2-7 Hz.*

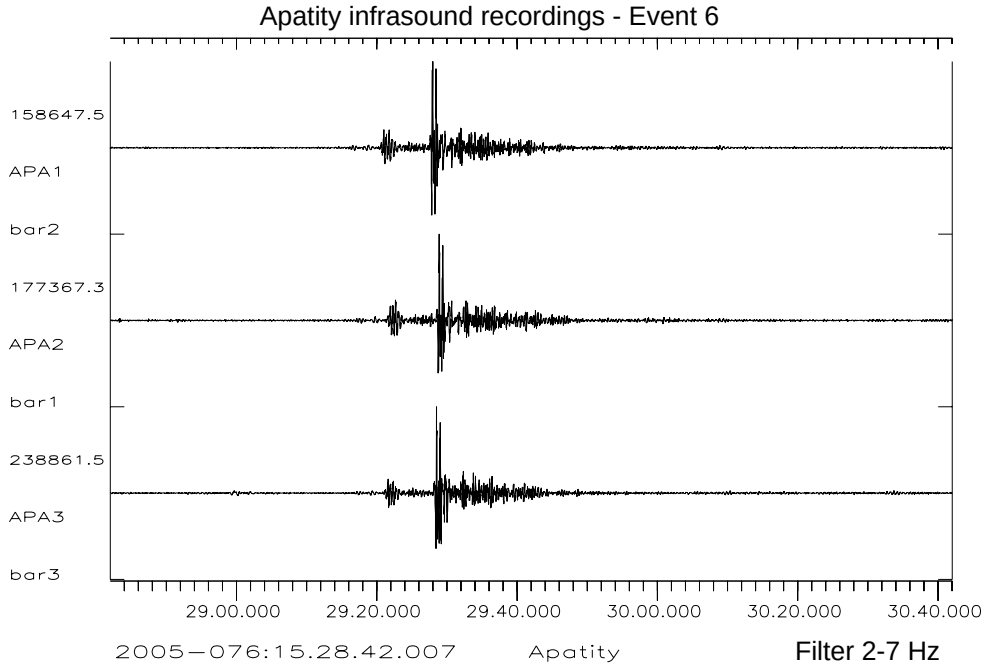

Fig. 6.4.11. *Apatity infrasound recordings of Event 6 in the database. The data are filtered in the frequency band 2-7 Hz.*

Location estimation

Although we do not know the exact coordinates of the explosion site, we have used this opportunity to investigate the stability of azimuth estimates of sound waves, using various subconfigurations of the ARCES array. These subconfigurations were:

1. The full ARCES array (A0, A,B,C and D-ring). 25 sensors. Diameter 3 km.
2. A0, A,B, and C-ring. 16 sensors. Diameter 1.5 km
3. A0, A,B ring. 9 sensors. Diameter 0.7 km.
4. A0, A-ring. 4 sensors. Diameter 0.3 km.

Table 6.4.2 shows the results of this analysis, as well as the corresponding results for the array of infrasound sensors at the Apatity array (3 sensors, diameter 0.4 km).

From the table, we see that the estimates were very stable, even for the smallest subset of the array (configuration 4, with a diameter of only 300 m). The estimates ranged from about 82 to about 86 degrees, with no significant change in the stability with the size of the selected array subset. For the 3-element APATITY infrasound array, (diameter 400 m), the estimates were likewise stable, ranging from 346 to 351 degrees.

We used the estimated azimuths (from the infrasonic waves) for the two arrays to locate the six events, using the HYPOSAT program (Schweitzer, 2001). For the Apatity array, we used the three infrasonic sensors, and for the ARCES array we used subconfiguration 2 above, which has a diameter close to that of the planned IS37 infrasound array. Fig. 6.4.12 shows the location results compared to those obtained using standard seismic analysis. As can be seen from the figure, the locations match quite closely. At this stage, we have not attempted to combine the seismic and infrasonic information to provide joint location estimates, since it is not clear how the individual observations should be weighted in order to obtain the best solution.

6.4.4 Conclusions and future plans

We have obtained some interesting results when comparing location estimates based on seismic and infrasonic recordings of surface explosions at local and regional distances. Using ARCES and Apatity array recordings of a set of explosions near the Norwegian-Russian border, we have found that the infrasonic locations (using azimuths only) match closely the locations obtained through standard seismic data analysis. This indicates an interesting potential for joint two-array infrasonic processing, and we recommend that this concept be further developed once the IMS infrasound array near ARCES has been established (expected in 2006).

An important task which we have not yet addressed is the development of an infrasonic real time signal detector. Several such detectors are available in various institutions, and we intend to build on this experience when designing the detector. Among the topics to be considered are which detection algorithm to select (e.g. Fisher detector, correlation detector, STA/LTA). We also need to find one or more filter bands for optimum processing, and define time windows for processing and f-k analysis.

The detector output will be similar to what is produced today for the seismic detectors. A phase association procedure will be implemented, attempting to associate the detected phases to seismic events detected by the regional network. The Generalized Beamforming (GBF) algorithm

(Ringdal and Kværna, 1989) will be used in the phase association procedure. We expect to have a number of unassociated detections, (i.e. detections by infrasound data only), and it will be a challenging task to combine these detections so as to define new "infrasonic" events.

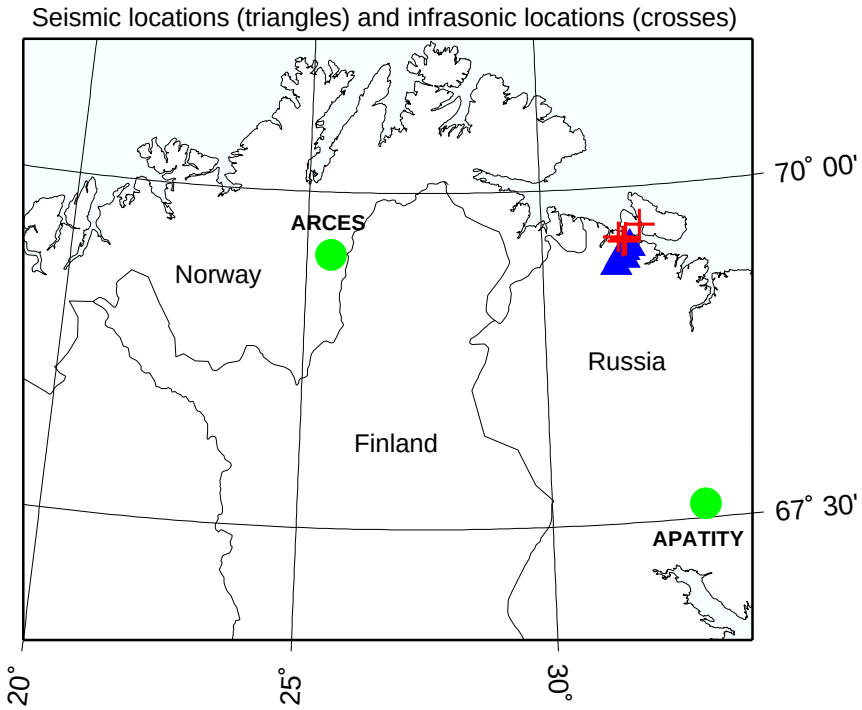

Fig. 6.4.12. *Map showing the location of the Apatity and ARCES arrays (marked as green), together with results from locating the six explosions described in the text. The triangles are locations based on standard interactive analysis of the seismic data from the ARCES and APATITY arrays, whereas the crosses are locations obtained using only the estimated azimuths of the sound waves recorded by the two arrays.*

Finally, it will be important to establish an interactive analysis tool and integrate the analysis with that currently done for the seismic data. Our preliminary aim is to augment the existing NORSAR regional seismic bulletin (analyst reviewed) with infrasound observations.

After the projected infrasonic array (IS37) in Karasjok, northern Norway, is installed, we plan to carry out joint processing of data from these two arrays. Further perspectives include cooperation with colleagues in Sweden, Netherlands and Germany for more extensive joint processing.

Acknowledgement

The Kola Regional Seismological Centre operates the Apatity seismic/infrasound array, and provided seismic and infrasonic waveforms from the array for this study.

References

Ringdal, F. and T. Kværna (1989). A multichannel processing approach to real time network detection, phase association and threshold monitoring, *Bull. Seism. Soc. Am., 79*, 1927-1940.

Ringdal, F. and T. Kværna (2004): Some aspects of regional array processing at NORSAR, *Semiannual Technical Summary, 1 July - 31 December 2003*, NORSAR Sci. Rep. 1-2004, Norway

Schweitzer, J. (2001): HYPOSAT - An Enhanced Routine to Locate Seismic Events, PAGEOPH 158, 277-290

Vinogradov, Yu. and F. Ringdal (2003). Analysis of infrasound data recorded at the Apatity array, *Semiannual Technical Summary 1 July - 31 December 2002*, NORSAR Sci. Rep. 1-2003, Kjeller, Norway.

Frode Ringdal
Johannes Schweitzer